Populations in Spatial Equilibrium*

Matthew Easton and Patrick W. Farrell†

This Version: August 2024

Abstract

Power law-like distributions for city populations are a distinctive, recurring feature of human settlement patterns. We propose a novel explanation for this phenomenon that reflects the qualities of a place (fundamentals) and its ability to benefit from trade based on its location (market access), two important forces that have not simultaneously been incorporated into an explanation of the city size distribution. Using random variation in geography to model these two terms within a quantitative spatial model results in lognormal population distributions which appear to follow a power law for the most populous locations (i.e., cities).

JEL Codes: R12, R13, F10, C31, C6.

*The authors thank Arslan Ali, Nadia Ali, Costas Arkolakis, Pierre-Philippe Combes, Donald Davis, Richard A. Davis, Jonathan Dingel, Thibault Fally, Madeline Hansen, Raphael Lafrogne-Joussier, Serena Ng, Eshaan Patel, Stephen Redding, Frédéric Robert-Nicoud, Andrés Rodríguez-Clare, Esteban Rossi-Hansberg, Bernard Salanié, Lin Tian, Conor Walsh, David Weinstein, Natalie Yang, and seminar participants at Columbia University and the 2024 European Meeting of the Urban Economics Association for helpful comments and discussions. Easton acknowledges the Program for Economic Research at Columbia University and the Alliance Doctoral Mobility Grant from Columbia University and Sciences Po for support.

†Easton: Columbia University (email: me2713@columbia.edu). Farrell: Columbia University (email: pwf2108@columbia.edu).

1 Introduction

The most remarkable empirical regularity in spatial economics is that the upper tail of the city size distribution appears to follow a power law, a phenomenon often referred to as Zipf's Law. Why this regularity arises is a question that quantitative spatial models, which form the basis of modern spatial economics, have thus far failed to answer. While a key feature of these models is their ability to recover the unobserved qualities or "fundamentals" of each location that rationalize the observed populations, they do not explain why the underlying fundamentals of locations and their market access should consistently generate the characteristic city size distribution. By contrast, existing explanations of Zipf's Law are inconsistent with quantitative spatial models. For example, these explanations either allow no role for a location's characteristics (Brakman et al. 1999; Rante et al. 2024), no role for a place's interactions with other locations (Lee and Li 2013; Behrens and Robert-Nicoud 2015), or no role for either factor to determine a city's population (Gabaix 1999b). That is, the literature that models the forces shaping cities cannot explain the regularity of the city size distribution, while the literature explaining city size distributions ignores the forces shaping cities.

Our paper provides a novel path out of this conundrum by showing that random variation in geography can generate the characteristic city size distribution within quantitative spatial models. Modeling the distribution of a location's fundamentals and its market access as resulting from random variation in local attributes and trade costs arising from geography, respectively, we show that both fundamentals and market access will be lognormally distributed. Together, these will generate a lognormal population distribution within quantitative spatial models. As a lognormal distribution approximates a power law in the upper tail our framework naturally generates the characteristic power law-like city size distribution. Our key advance is to show that random variation can generate a lognormal market access term due to the particular way market access is constructed within these models, advancing on prior work that has used random variation only to generate lognormally

distributed fundamentals.

The intuition for why random variation within and across space generates a lognormal population distribution relies on two applications of a central limit theorem. Within the Allen and Arkolakis (2014) model, we show that the population of each location can be expressed as the product of two terms. One term represents that location's market access and is written as a trade cost-weighted sum over all locations. The other term solely reflects that location's fundamentals, which are a function of that location's geographic attributes. Our major contribution is to model both the fundamentals and the trade costs influencing market access as the outcome of random geographic variation. We accomplish this in two steps. First, we provide a novel proof applying a result from Marlow (1967) for sums of positive random variables. We apply this result to the market access summation, where trade costs vary to reflect differences in geography, and demonstrate that it renders the market access terms lognormally distributed by a central limit theorem. Second, we model the locational fundamentals as multiplicative aggregates of randomly distributed geographic attributes. Since multiplicative processes are additive in logs, the locational fundamentals will also be lognormally distributed by a central limit theorem. The population distribution, a product of these two lognormal terms, will thus be lognormally distributed.

The separation of the explanation into two parts has attractive economic interpretations because there is substantial empirical evidence that both a place's characteristics and its location in space influence its population. Within quantitative spatial models, the former is reflected by a location's fundamentals and the latter by its market access. Our paper is the first to show how these forces *jointly* produce the distinctive population distribution. This result holds even allowing for other important economic forces captured by these models, such as agglomeration and congestion externalities, to influence the population distribution.

We simulate our model to test our framework's robustness and ability to match results in the theoretical and empirical literatures. We show that differences in local productivity spillovers, intra-city congestion externalities, and

inter-city transportation costs can explain variation in the city size distribution observed in data. We find that as agglomeration benefits rise the size distribution becomes more unequal, consistent with observed changes to the U.S. city size distribution (Gabaix and Ioannides 2004). Increasing inter-city transportation costs also results in a more unequal city size distribution. This provides a potential explanation for the very large "primate" cities and unequal city size distributions of developing countries, where domestic transportation costs are often much higher than in developed countries (Teravaninthorn and Gaël 2009; Atkin and Donaldson 2015).

Our paper touches on several branches of the spatial economics literature. Many theoretical explanations of the city size distribution are based on the similarly striking empirical observation that city growth rates often appear unrelated to city population, such as Gabaix (1999a), Gabaix (1999b), Blank and Solomon (2000), Eeckhout (2004), Rossi-Hansberg and Wright (2007), and Córdoba (2008).[1] However, the assumption of random growth is inconsistent with the empirical evidence on the distribution of cities in significant ways. The growth of cities does not appear random in many important cases, particularly following major shocks.[2] Random growth explanations also fail to capture the influence of the characteristics of a place on the attractiveness of producing or residing there, implying that the large populations of New York City, Tokyo, and London are random and unrelated to their advantageous geographies. These theories are also aspatial and do not allow for interactions between different locations to shape settlement patterns, failing to capture the contribution of trade to the scale of the aforementioned global cities.[3]

[1]Random growth is often referred to in the literature as Gibrat's law. The "law" is an application of the central limit theorem to the log of the product of independent shocks, originally formulated to describe the growth of firms (Gibrat 1931).

[2]Notable instances of recovery from shocks are documented in Davis and Weinstein (2002), Brakman et al. (2004) and Davis and Weinstein (2008) following bombings, and in Johnson et al. (2019) following pandemics. Desmet and Rappaport (2017) also document the absence of the random growth phenomenon for cities during the settlement of the American West.

[3]New York City is located on one of the largest natural harbors on Earth and its much greater population relative to Lost Springs, Wyoming—the 2020 population ratio was 8,804,190 to 6—is likely related to New York's favorable geography and the benefits

There are papers within the literature on city size distributions that have accounted for either the role of a place's characteristics or its location in determining its population, but our paper is the first to include both of these important forces simultaneously. Papers that do account for the importance of geography or fundamentals, such as Lee and Li (2013) and Behrens and Robert-Nicoud (2015), have lacked trade between locations. In contrast, those papers which account for the importance of trade and market access, such as Brakman et al. (1999) and Rante et al. (2024), are models without differentiated geographies which consist of identical locations. By placing our explanation for the distribution's emergence within a quantitative spatial model, we can include roles for both local characteristics and trade between locations. Further, given the properties of quantitative spatial models, we also demonstrate that population distributions will exhibit random growth in equilibrium in response to increases in the aggregate population level. This provides consistency with the observation of random growth in many contexts that motivated prior models.

By integrating the literature on population distributions with that on quantitative spatial models, we show the conditions under which these models generate the characteristic city size distribution. Models of the spatial economy, beginning with Krugman (1991), Helpman (1998), and Fujita et al. (1999), highlight the roles of space, local spillovers, and the importance of trade between locations in determining population distributions. The spatial literature is now based on quantitative spatial models as developed in Allen and Arkolakis (2014), Redding (2016) and Redding and Rossi-Hansberg (2017). The literature on quantitative spatial models suffers from much the opposite problem than that afflicting the literature on the city size distribution. While quantitative spatial models incorporate many of the forces that influence the size of cities, they do not explain the regularity of the population distribution. These models can recover the unobserved qualities of each location, their "fundamentals," which rationalize observed populations. Yet this inversion is possible for

of its location for trade. Some attributes of landlocked Lost Springs include its low annual precipitation and a coal mine which last operated in the 1930s.

any arbitrary vector of "populations," even those with little resemblance to real-world population distributions.[4] We demonstrate how both heterogeneity in the attributes of different places and trade across space will generate lognormal population distributions in equilibrium as a result of random variation in geography.[5] Thus, we show how the models within this literature can be used to provide a deep explanation for why the population tends to be distributed in a particular way within countries. As our result relies solely on variation in geography and applications of a central limit theorem within these models, its simplicity and generality can explain the consistent observation of this phenomenon in many contexts.

Our framework also provides a strong theoretical link between observable characteristics of the world, which a broad literature demonstrates are important for local populations, and the entire city size distribution. The largest cities around the world tend to be in locations that are good for production and offer quality-of-life benefits to residents. The literature has found a large role for such "first-nature" geographic characteristics in explaining local populations, as in Rappaport and Sachs (2003), Nordhaus (2006), Nunn and Puga (2012), Henderson et al. (2018), Bosker and Buringh (2017), and Alix-Garcia and Sellars (2020). We show that embedding fundamentals modeled as in Lee and Li (2013) and Behrens and Robert-Nicoud (2015), which reflect local geographic characteristics, within a quantitative spatial model will result in realistic population distributions, extending the aspatial results of those papers to a spatial setting. Further, basing the origin of the population distribution on slow-changing geography can explain the persistence and resilience of the city size distribution to negative shocks.[6]

The paper proceeds as follows. Section 2 argues that populations are best

[4] Adão et al. (2023) make a similar point, noting that modern spatial models are saturated with free parameters such that they are always able to exactly match the underlying data.

[5] We also show that the exogenous locational fundamentals recovered in Allen and Arkolakis (2014) appear lognormal, supporting our modeling of fundamentals as lognormally distributed. We discuss this further in Section 3 and Supplemental Appendix C.8.

[6] Davis and Weinstein (2002) propose geography as a likely determinant of the population distribution, given the recovery of the cities to their prior place in the population distribution following devastating bombings.

described by a lognormal distribution and establishes the link between this distribution and the appearance of a power law for cities. Section 3 presents a standard quantitative spatial model and shows that, given the structure of the equilibrium condition, a lognormal population distribution results from both trade across space and random variation in geography within places. Section 4 demonstrates that the model captures several results in the empirical literature on city size distributions via simulation. Section 5 concludes.

2 Seeing a Power Law in Populations

The appearance of a power law-like distribution for city populations is a well-documented feature of human geography. As articulated in Gabaix (1999b), the regularity of its appearance across countries, the definition of a "city," and time means it can reasonably be held as a minimum criterion for a model of cities. This distribution is typically illustrated with a simple plot and accompanying regression. For some truncation of the population distribution to include only the most populous locations ("cities"), the plot of the log population rank of a city and the log population of the city often appears strikingly linear and regression given by:

$$\ln(city\,rank_i) = \theta_0 + \theta_1 \ln(city\,pop_i) + \epsilon_i \tag{1}$$

for many countries delivers a high R^2 and frequently an estimate for θ_1 near -1, as in Figure I for U.S. cities. This slope is characteristic of a specific power law referred to as Zipf's Law, which can be stated as the largest city in a given country being n times the size of the n^{th}-largest city. Interpreting this regression as describing the true city size distribution would mean that city populations follow a Pareto distribution with shape parameter $\alpha_P = 1$ and minimum city size x_m, reflecting the choice of truncation point.[7]

[7]The estimate of $\theta_1 = -1$ means the power law is such that for size X, the probability that a city is larger than X is proportional to $\frac{1}{X}$. A Pareto distribution with shape parameter $\alpha_P = 1$ and minimum city size x_m gives the necessary $P(x > X) = \frac{x_m}{X}$, which is the Pareto counter-cumulative distribution function for this α_P. The link between the (log) rank-size

Figure I:
An Apparent Power Law for U.S. Cities in 2020

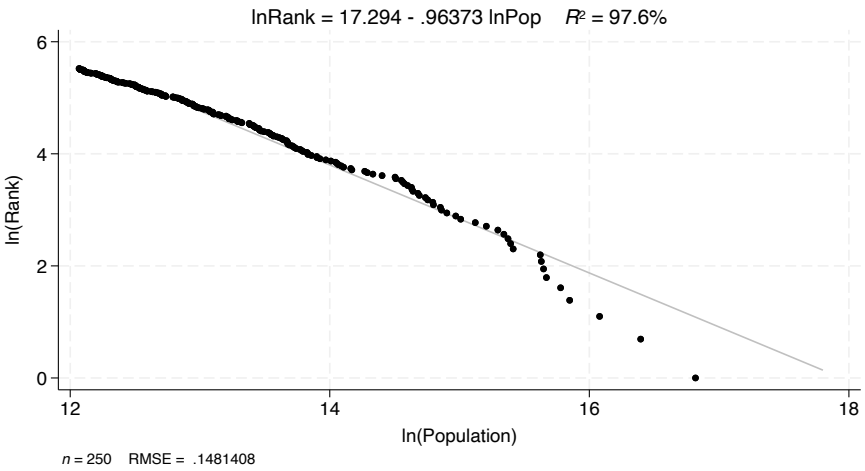

Notes: The appearance of a power law for top 250 U.S. metropolitan statistical areas (MSAs) in 2020.
Data Source: U.S. Census

Instead of being a true power law, the city size distribution may result from cities being a subset of a full population distribution which appears similar to a Pareto distribution for tail observations. Eeckhout (2004) demonstrates that the full population distribution for the U.S. appears lognormal. We construct an update to one of the key figures of Eeckhout (2004) in Figure II, which shows that this continues to hold for the U.S. in 2010. The left panel shows a histogram of log population, which closely matches the overlaid normal distribution matching the mean and standard deviation of the empirical distribution, and the right panel shows close fit to the normal distribution in a quantile-quantile (QQ) plot. The tail of a lognormal distribution often appears similar to a Pareto distribution, which can be understood by considering the lognormal PDF:

$$f(x) = \frac{1}{x\sigma\sqrt{2\pi}} \exp\left(-\frac{(\ln(x)-\mu)^2}{2\sigma^2}\right) \tag{2}$$

plot and the Pareto distribution is established in more detail in Gabaix (2009).

Figure II:
Log Population, U.S. Census Places in 2010

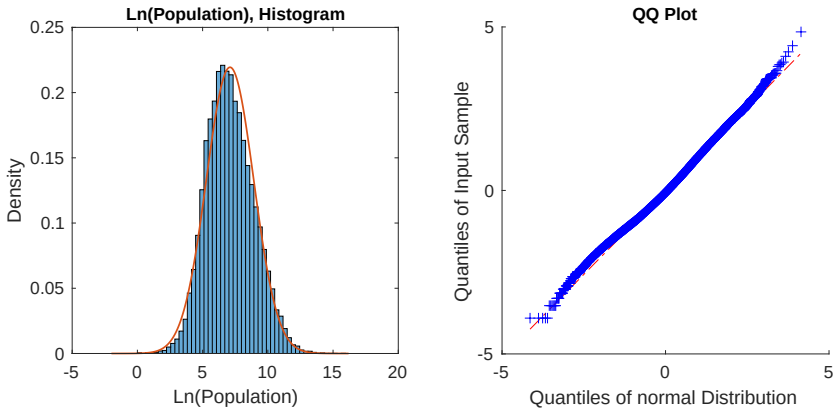

Notes: The left panel is a histogram of log population for U.S. incorporated places and census designated places in 2010, with an overlaid normal distribution matching the moments of the empirical log distribution. The left panel shows a QQ plot of the (normalized) empirical population distribution against a standard normal distribution. The fit of the log population to the normal distribution distribution means the population distribution appears lognormal. This right panel of this figure is an update to Figure 2 of Eeckhout (2004), which uses data from the 2000 Census.
Data Source: U.S. Census

After some algebra (given in Supplemental Appendix A.1), this can be rewritten as:

$$f(x) = \Gamma_{LN} x^{-\alpha(x)-1} \tag{3}$$

where $\Gamma_{LN} = \frac{1}{\sigma\sqrt{2\pi}} \exp\left(-\frac{\mu^2}{2\sigma^2}\right)$ and $\alpha(x) = \frac{\ln(x)-2\mu}{2\sigma^2}$. Contrast this with the density function of a Pareto distribution:

$$j(x) = \Gamma_P \, x^{-\alpha_P - 1} \tag{4}$$

where $\Gamma_P = \alpha_P x_m^{\alpha_P}$ and the minimum city population is denoted x_m. The log-normal PDF in Equation 3 is similar to the Pareto density function in Equation 4, but with a scale-varying "shape parameter"-like term. As Malevergne et al. (2011) show, provided the σ parameter is not too small, the value $\alpha(x)$ takes in the right tail will be stable over much of the tail distribution as $\alpha(x)$ grows

logarithmically in x.

The Pareto interpretation of the tail of the population distribution appears dominant in the literature despite its limitations and the strict assumptions it necessitates. First, the Pareto distribution is taken to apply to only a subset of large settlements and not the full population distribution. This requires truncating a data series with no obvious truncation point. Early studies were limited to only the largest cities or settlements because of the comparative ease of accessing population counts for the largest places.[8] With more complete data on population distributions, the choice of a truncation point to support the Pareto interpretation becomes critical and there is no widely accepted method for determining such a cutoff. Many researchers rely on a visual test of the data to determine a cutoff (Gabaix 2009). Second, beyond the need to truncate the data to fit a Pareto distribution, models generating a Pareto population distribution must rely on strong assumptions regarding city growth dynamics. For example, Gabaix (1999b) obtains a Pareto distribution by assuming that cities cannot fall below a certain minimum size such that the otherwise random growth process is "reflected" at the lower bound. Third, the systematic deviations of the far right tail below the Pareto distribution observed in many countries (evident in Figure I for the U.S.) are very large in magnitude, which is obscured by the log-log scale. In Supplemental Appendix B, we show that the estimated Pareto exponent implies a cumulative absence of nearly 76 million people from the 250 U.S. MSAs in Figure I in expectation, roughly a quarter of the U.S. population.[9]

The lognormal interpretation's attractive properties stand in direct contrast to the shortcomings of the Pareto. The lognormal distribution appears to fit both the body of the population distribution as well as the right tail,

[8]This is true of early work, such as Auerbach (1913) and Zipf (1949). While Auerbach had data on many small settlements, a table in his paper includes just the 94 largest; see the recent translation in Auerbach and Ciccone (2023). Even more recent investigation of Zipf's Law in Krugman (1996), for instance, included just the top 135 cities as the *Statistical Abstract of the United States* included only those cities (Eeckhout 2004).

[9]Alternative estimates of the power law based on different truncation points imply as many as 500 million "missing" people in the largest U.S. MSAs, substantially more than the entire U.S. population, which we discuss in Supplemental Appendix B.

obviating the need for arbitrary truncation. Further, the scale-varying "shape parameter"-like term of the lognormal (as shown in Equation 3) can explain commonly observed deviations in real-world city size distributions. The likelihood of very large cities is lower when the true distribution is lognormal than for a similar Pareto, because the scale-varying "shape parameter"-like term is increasing in x. This appears to match the global city distribution (Rossi-Hansberg and Wright 2007), as the largest cities in most countries tend to fall below the slope of the fitted regression line.[10] Other features of real-world population distributions, such as the sensitivity of the estimated slope to the choice of truncation point, are consistent with the lognormal distribution as well.[11]

The appearance of a power law-like city population distribution is likely the result of focusing on the tail of a lognormal full population distribution. Such an interpretation requires fewer restrictive assumptions and appears to better fit the observed data, both in the body of the population distribution (which is necessarily ignored by the Pareto interpretation) and in the tail (which behaves more lognormal than Pareto). In the following sections, we demonstrate that the equilibrium population distribution within many spatial models is lognormal given a realistically modeled geography.

[10]Proponents of the Pareto interpretation have attempted to accommodate this divergence by arguing that the forces acting on small cities are different from those acting on large cities, generating different power laws for different sizes of cities. A lognormal distribution naturally exhibits this deviation without the need to treat subsets of the distribution differently. We provide a further discussion of the scale variance of the lognormal distribution and its contrast with the Pareto distribution in Supplemental Appendix B.

[11]This property is discussed at length in Eeckhout (2004) and demonstrated in Supplemental Appendix Figure A.II where we expand or reduce the number of cities relative to Figure I. The sensitivity to the truncation point and the lack of a reliable rule for truncating the distribution suggest that the frequently estimated -1 exponent is unlikely to be a meaningful feature of the data. For some truncation of tail observations drawn from many lognormal distributions, the log-rank log-population plot will appear to take a slope of -1 as the exponent in Equation 3 diverges smoothly.

Figure III:
An Example Circular Geography

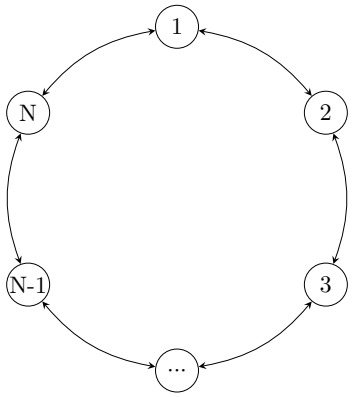

Notes: An illustrative example of the circular geography we consider in the main text. Locations $i \in \mathcal{N}$ are arrayed around a circle and trade occurs along the perimeter of the circle.

3 Lognormal Populations in Spatial Models

We now describe a canonical quantitative spatial model within which we demonstrate our key result. We use a discretized version of the model in Allen and Arkolakis (2014), which nests a broad class of spatial models, and show that a realistic modeling of geography and trade will lead to lognormal population distributions in equilibrium.[12]

3.1 A Quantitative Spatial Equilibrium Model

The world consists of locations indexed by $i \in \mathcal{N}$, where $\mathcal{N} = \{i \mid i \in \mathbb{N}, 1 \leq i \leq N\}$. The index i reflects each location's position in a one-dimensional geography arranged as a circle. An example of the geography is included in Figure III. We adopt a circular geography here to simplify the exposition but we show in Supplemental Appendix A.5 that our result generalizes to a two-dimensional Euclidean space.[13]

[12]The Allen and Arkolakis (2014) model is based on the two location model presented in Helpman (1998), generalized to an arbitrary number of locations.

[13]In our simulated results we also use a two-dimensional geography.

We assume that adjacent locations are evenly spaced at a distance of 1 around the circumference of the circle. The distance between any pair of locations $i, n \in \mathcal{N}$, $i \neq n$, denoted $\delta_{i,n}$, is the minimum distance around the circumference of the circle between the two locations in either the clockwise or counterclockwise direction. Without loss of generality, assume that $i \leq n$. Then we can write the minimum distance traveled $\delta_{i,n}$ as

$$\delta_{i,n} = \min(\underbrace{n - i}_{clockwise} , \underbrace{N - n + i}_{counterclockwise}). \tag{5}$$

The distance between locations is important for accurately reflecting correlations across space which often depend on distance. The similarities of locations nearby in space reflects the "first law of geography," formulated by Tobler (1970) as "everything is related to everything else, but near things are more related than distant things."

Trade between locations is costly, and trade costs are related to but distinct from distance. Travel between adjacent locations incurs a cost t_i, defined such that t_i for $i \in \{1, 2, ..., N-1\}$ is the cost of traveling over the segment between i and $i+1$ and for $i = N$ is the cost of traveling over the segment between N and 1. All t_i are strictly positive and finite-valued random variables drawn from some common distribution, reflecting variation in geography whereby traversing some geographies is more difficult than traversing others. The realized trade costs $\tau_{i,n}$ between any pair of locations $i, n \in \mathcal{N}$, assuming without loss of generality that $i \leq n$, is the minimum trade cost when summing over the realized travel costs around the circle in the clockwise and counterclockwise directions between the two locations:

$$\tau_{i,n} = 1 + \min \left(\sum_{j \in A} t_j \, , \sum_{k \in B} t_k \right), \quad A = \{j | j \in \mathcal{N}, j \in [i, n)\}, B = \{k | k \in \mathcal{N}, k \notin A\}. \tag{6}$$

This structure imposes symmetric iceberg trade costs such that $\tau_{i,i} = 1$ for all $i \in \mathcal{N}$, $\tau_{s,t} = \tau_{t,s}$, $\tau_{s,t} > 1$ for $s \neq t$, and ensures that trade costs between any pair of locations $s, t \in \mathcal{N}$ are bounded above by a positive num-

ber. The circle geography ensures all locations face the same expected average trade costs. By construction, expected trade costs between locations are increasing in distance but reflect a notion of "effective" distance relevant for trade between locations rather than measured geographic distance relevant for considering the similarity of nearby locations.

Each location has an exogenous productivity fundamental A_i and an exogenous amenity fundamental U_i, both of which are strictly positive, real-valued random variables drawn from some probability distribution. We discuss the fundamentals further later in this section, where we argue that these should reflect variation in the geographic attributes of a place and the spatial correlation patterns of attributes across space. A location's effective productivity and amenity value may also be affected by negative or positive externalities due to the local population L_i. We define the "composite fundamentals" as:

$$\tilde{A}_i = A_i L_i^{\alpha} \tag{7}$$

$$\tilde{U}_i = U_i L_i^{\beta} \tag{8}$$

where the typical case will consist of $\alpha > 0$ and $\beta < 0$, reflecting positive productivity spillovers from agglomeration and the negative impact of overcrowding on amenities. Geography within this model is represented by the set of functions defining the locational fundamentals, $\tilde{A}_i$ and $\tilde{U}_i$, along with the trade costs function τ defining the spatial relationship between locations in the model.

We make the Armington assumption that each location produces a differentiated good. There is a population of homogeneous workers $\bar{L} \in \mathbb{R}_{++}$ who can freely move to any location. Workers have common constant elasticity of substitution preferences over goods in their welfare function given by:

$$W_i = \left(\sum_{n \in \mathcal{N}} q_{n,i}^{\frac{\sigma-1}{\sigma}} \right)^{\frac{\sigma}{\sigma-1}} \tilde{U}_i \tag{9}$$

where $\tilde{U}_i$ is the composite amenity fundamental of location i and $q_{n,i}$ denotes

the total consumption in i of the good produced in n and $\sigma > 1$ governs the elasticity of substitution.

Production is perfectly competitive.[14] A worker in location i can produce $\tilde{A}_i$ units of the local differentiated good, where $\tilde{A}_i$ is the composite productivity fundamental of location i. The number of workers and wages in a location are given by the functions $L : N \to \mathbb{R}_{++}$ and $w : N \to \mathbb{R}_{++}$.[15]

Based on the CES assumption, we can write the amount of each good produced in any location i consumed in location n as:

$$q_{i,n} = Q_n \left(\frac{p_{i,n}}{P_n} \right)^{-\sigma} \tag{10}$$

where Q_n is aggregate consumption in n, $Q_n = \frac{w_n L_n}{P_n}$, and P_n is the price index in location n, given by:

$$P_n = \left(\sum_{i \in \mathcal{N}} p_{i,n}^{1-\sigma} \right)^{\frac{1}{1-\sigma}} \tag{11}$$

Given the assumption of perfect competition the price of the good produced in i consumed in n, can be expressed as:

$$p_{i,n} = \frac{\tau_{i,n} w_i}{\tilde{A}_i} \tag{12}$$

Combining the quantity (Equation 10) and price (Equation 12) expressions, we can write the value of the good produced in i consumed by n as:

$$X_{i,n} = \left(\frac{\tau_{i,n} w_i}{\tilde{A}_i P_n} \right)^{1-\sigma} w_n L_n \tag{13}$$

By the CES assumption we can express the welfare of a worker in each location as:

$$W_i = \frac{w_i}{P_i} \tilde{U}_i \tag{14}$$

[14] This model nests cases of monopolistic competition, as demonstrated in the appendix to Allen and Arkolakis (2014).

[15] No location will be unpopulated or offer zero wages in equilibrium given the range of parameters we consider.

The value of income in a location must be equal to the value of production:

$$w_i L_i = \sum_{n \in \mathcal{N}} X_{i,n} \tag{15}$$

The labor market clears:

$$\sum_{n \in \mathcal{N}} L_n = \bar{L} \tag{16}$$

We can then combine the welfare expression (Equation 14), value of consumption expression (Equation 13), and income expression (Equation 15) to get:

$$L_i w_i^{\sigma} = \sum_{n \in \mathcal{N}} W_n^{1-\sigma} \tau_{i,n}^{1-\sigma} \tilde{A}_i^{\sigma-1} \tilde{U}_n^{\sigma-1} L_n w_n^{\sigma} \tag{17}$$

The welfare expression (Equation 14) combined with the price index and and prices (Equations 11 and 12) yields:

$$w_i^{1-\sigma} = \sum_{n \in \mathcal{N}} W_i^{1-\sigma} \tau_{n,i}^{1-\sigma} \tilde{A}_n^{\sigma-1} \tilde{U}_i^{\sigma-1} w_n^{1-\sigma} \tag{18}$$

Given the form of the externalities in Equations 7 and 8, free movement between locations which ensures worker welfare is equal in all locations ($W_i = \bar{W}$ for all i), and symmetric trade costs we can combine Equations 17 and 18 into a single equation given by:

$$\bar{W}^{\sigma-1} L_i^{\tilde{\sigma}\gamma_1} = A_i^{\tilde{\sigma}(\sigma-1)} U_i^{\tilde{\sigma}\sigma} \sum_{n \in \mathcal{N}} \tau_{n,i}^{1-\sigma} U_n^{\tilde{\sigma}(\sigma-1)} A_n^{\tilde{\sigma}\sigma} \left(L_n^{\tilde{\sigma}\gamma_1} \right)^{\frac{\gamma_2}{\gamma_1}} \tag{19}$$

where:

$$\tilde{\sigma} = \frac{\sigma - 1}{2\sigma - 1}, \quad \gamma_1 = 1 - \alpha(\sigma - 1) - \beta\sigma, \quad \gamma_2 = 1 + \alpha\sigma + (\sigma - 1)\beta$$

The existence and uniqueness of the equilibrium, and a mechanism for finding it, are established in Allen and Arkolakis (2014) when $\frac{\gamma_2}{\gamma_1} \in (-1, 1]$ (the discrete case is considered in their online appendix). We focus on this part of the parameter space in our simulated results, which occurs when $\alpha + \beta \leq 0$

and is the empirically relevant case, but our result does not depend on this inequality. For any realization of fundamentals and trade costs we thus can recover a unique vector of populations.

In the following subsections we demonstrate that the equilibrium population within this model will be lognormally distributed given a realistic modeling of the fundamentals and trade costs based on variation in geography. We begin by rewriting Equation 19 in terms of the population in each location i in simplifying notation as:

$$L_i = \Omega_i \left(S_i\right)^{\frac{1}{\tilde{\sigma}\gamma_1}} \tag{20}$$

where $\Omega_i = \left(\bar{W}^{1-\sigma} A_i^{\tilde{\sigma}(\sigma-1)} U_i^{\tilde{\sigma}\sigma}\right)^{\frac{1}{\tilde{\sigma}\gamma_1}}$, which we refer to as the "own-fundamental" term as it consists only of location i's fundamentals and the common positive constant $\bar{W}$, and $S_i = \sum_{n \in \mathcal{N}} s_{n,i}$ with $s_{n,i} = \tau_{n,i}^{1-\sigma} U_n^{\tilde{\sigma}(\sigma-1)} A_n^{\tilde{\sigma}\sigma} L_n^{\tilde{\sigma}\gamma_2}$, which we refer to as the "market access" term of location i as it is a trade cost-weighted sum over all locations $n \in \mathcal{N}$. Each term $s_{n,i}$ of this summation represents the contribution of location n to the market access of location i.

We now demonstrate that, given a realistic modeling of variation in geography across space and within a place, both of these terms will be lognormally distributed. This will allow us to show that the equilibrium population also follows a lognormal distribution.

3.2 Variation over Space and the Distribution of Market Access

We first show that the distribution of the market access term, which is a summation over positive random variables, converges in distribution to a lognormal. This result follows from the application of a central limit theorem that allows for a particular type of dependence structure across elements of the summation that is likely to hold in spatial contexts and a useful lemma due to Marlow (1967) for sums of positive random variables.

The market access term for each location i given by $S_i = \sum_{n \in \mathcal{N}} s_{n,i}$, consists of a summation over the random variables $s_{n,i}$, each a function of the

random variables $\tau_{n,i}$, A_n, U_n, and L_n, for all $n \in \mathcal{N}$.[16] Many central limit theorems apply only to independent and identically distributed random variables, but the sequences given by $\{s_{n,i}\}$ are unlikely to consist of i.i.d. random variables. The fundamentals of a location are intended to reflect its geographic advantages, as we argue in more detail in the following section, and as geography is similar for nearby locations the productivity and amenity fundamentals A_i and U_i are unlikely to be independent for nearby locations. Further, a location near a highly populous city will (provided trade costs are not prohibitive) benefit from access to the market of its neighbor such that the populations L_i of nearby locations are also unlikely to be independent. Lastly, trade costs between any i to any two other adjacent locations $j, j+1$, $\tau_{j,i}$ and $\tau_{j+1,i}$, will tend to be similar by construction as they differ by at most t_j, the trade cost of traversing the additional interval between j and $j+1$.

Despite the potential for correlations among nearby locations, we argue that over long distances the fundamentals, populations, and trade costs should approach independence. Nearby locations often have broadly similar geographic attributes, like the climatic similarities of New York City and northern New Jersey, but this spatial correlation declines with distance such that New York City is quite dissimilar from both Monterrey, Mexico, and Nuuk, Greenland.[17] As such, we assume that while fundamentals may be similar for nearby locations they may also differ substantially over greater distances. Trade costs between i and any pair of locations $j, k \neq i$, given by $\tau_{j,i}$ and $\tau_{k,i}$, may also differ substantially when the distance between k and j is large since trade costs are not a pure function of distance but rather reflect random variation in the difficulty of travel. Rugged mountains may separate some nearby locations while other distant locations have gentle plains between them. As such, it is possible that while $\delta_{j,i} < \delta_{k,i}$ such that i is closer geographically to j than to k, travel from i to k occurs clockwise around the circular geography and is,

[16] In Supplemental Appendix A.4, we motivate the treatment of $s_{n,i}$ and L_n as random variables, because each L_n is an element of a random sequence corresponding to the eigenvector of a random matrix.

[17] Nuuk and Monterrey are roughly equidistant from New York City, both at a distance of 1,850 miles.

due to random variation in trade costs, substantially easier than travel in the counterclockwise direction from i to j such that $\tau_{j,i} \gg \tau_{k,i}$. Given independence in fundamentals and trade costs over long distances, the distribution of population can also be reasonably assumed to approach independence as distance increases. As such, for each i the realizations of $s_{j,i}$ and $s_{k,i}$, for locations $j, k \in \mathcal{N}$ are likely to near independence as distance between j and k increases.

Many modern central limit theorems allow for precisely this type of asymptotic independence. The formal assumption we must impose in order to apply a central limit theorem is that the sequences must be α-mixing for each $i \in \mathcal{N}$.[18] A formal definition of α-mixing for sequences is given in Supplemental Appendix A.3. The concept requires that all events defined on arbitrary subsets of an α-mixing sequence approach independence as the "distance" between the subsets increases, where distance is reflected in the index of the sets. This concept is often used in the analysis of time series, where the index reflects the timing of the observation and imposes a natural concept of the distance between elements of the sequence.

In our setting, we also have a natural concept of distance, $d_{n,i}$. We can re-index the elements of the sequence $\{s_{n,i}\}$ in terms of distance by defining for each i an alternative sequence ordered by distance from i, $\{s^d_{j,i}\}$, where $s^d_{1,i} = s_{i,i}$ (at a distance of 0) is followed by $s^d_{2,i} = s_{i+1,i}$, $s^d_{3,i} = s_{i-1,i}$ (both at a distance of 1), and so on.[19] Note that as the sequences $\{s^d_{j,i}\}$ are simply a re-indexing of the sequences $\{s_{n,i}\}$, $S_i = \sum_{n\in\mathcal{N}} s_{n,i} = \sum_{j\in\mathcal{N}} s^d_{j,i}$ for all $i \in \mathcal{N}$. We assume that the sequences $\{s^d_{j,i}\}$ are α-mixing for all $i \in \mathcal{N}$ to reflect asymptotic independence with respect to distance.

Lemma 1 is a central limit theorem for α-mixing sequences due to Herrndorf (1984), introduced to the spatial economics literature by Lee and Li (2013). It allows us to demonstrate convergence of a sum over a sequence of non-i.i.d random variables to a normal distribution, provided asymptotic independence

[18] This concept is also referred to as "strong mixing" or "weak dependence."

[19] Given that N is adjacent to 1 in the indexing within the circular geography, when considering $i = 1$ the value for $i - 1$ will be equal to N.

(α-mixing) and other moment conditions for the sequence.

***Lemma 1 (Herrndorf 1984)**: Let $\{x_i\}$ be an α-mixing sequence of random variables satisfying the following conditions:*

i. $\mathbb{E}[x_i] = 0, \forall i$

ii. $\lim_{n\to\infty} \frac{\mathbb{E}\left[(\sum_{i=1}^{n} x_i)^2\right]}{n} = \bar{\sigma}^2, 0 < \bar{\sigma}^2 < \infty$

iii. $\sup_{i\in\mathcal{N}} \mathbb{E}[x_i^b] < \infty$, *for some* $b > 2$

iv. $\sum_{s=1}^{\infty} (\alpha_s)^{1-\frac{2}{b}} < \infty$

Let $X_n = \sum_{i=1}^{n} x_i$. Then as $n \to \infty$, $\frac{1}{\sqrt{n}\bar{\sigma}} X_n$ converges in distribution to the standard normal distribution.

The proof of Lemma 1 is given in Herrndorf (1984), and discussion of the conditions is given in Lee and Li (2013). Lemma 1 allows us to apply a central limit theorem to the sums S_i for all $i \in \mathcal{N}$, provided the sequences $\{s_{n,i}^d\}$ fulfill the requirements of the lemma.

An additional property of the summations S_i allows us to move from a central limit theorem in levels to one in logs, which will allow us to characterize the distribution of S_i as lognormal. Each $s_{n,i}$ must be strictly positive, as A_n, U_n, $\tau_{n,i}$, and L_n are all strictly positive and so $s_{n,i} = \tau_{n,i}^{1-\sigma} U_n^{\tilde{\sigma}(\sigma-1)} A_n^{\tilde{\sigma}\sigma} L_n^{\tilde{\sigma}\gamma_2} > 0$. This allows us to apply a useful lemma from Marlow (1967), which provides conditions under which a lognormal distribution may appear from a summation of positive random variables:

***Lemma 2 (Marlow 1967)**: Let $\{X_n\}$ be a sequence of positive random variables. Suppose there exist sequences of positive real numbers $\{a_n\}$ and $\{b_n\}$, and a distribution F such that*

i. *At each point of continuity of F,* $\lim_{n\to\infty} P\left\{\frac{X_n - a_n}{b_n} \leq x\right\} = F(x)$

ii. $\lim_{n\to\infty} \left(\frac{b_n}{a_n}\right) = 0$

Then at each point of continuity of F, $\lim_{n\to\infty} P\left\{\left(\frac{a_n}{b_n}\right) \ln\left(\frac{X_n}{a_n}\right) \leq x\right\} = F(x)$

The proof of Lemma 2 is given in Marlow (1967). Condition (i) can reflect convergence under a central limit theorem (such as Lemma 1), where $F(x)$ is the standard normal distribution and the sequences a_n and b_n are the mean and standard deviation of some X_n resulting from a sum of random variables. Condition (ii) then necessitates that the coefficient of variation (the ratio of the standard deviation to the mean) of X_n is zero in the limit as n grows large. Many sums of positive random variables fulfill this requirement and examples are given in Supplemental Appendix A.2.

For a sum that satisfies the conditions for a central limit theorem and condition (ii), Lemma 2 states that the given normalization of the sum will converge in distribution to a lognormal random variable.[20] Lemma 2 is crucial for understanding the population distribution within many spatial equilibrium models, as these models often incorporate a notion of "market access" via a trade cost-weighted sum over all locations. All of the elements of these sums must be strictly positive, and provided these fulfill the conditions necessary for applying a central limit theorem and Lemma 2 the distribution of these "market access" terms will approach a lognormal distribution as the number of locations grows large. We state this result in Proposition 1.

Proposition 1: *For each $i \in \mathcal{N}$, define the sequences $\{s^d_{1,i}, s^d_{2,i}, ...s^d_{N,i}\}$ and the demeaned sequences $\{\hat{s}^d_{n,i}\}$ such that $\mathbb{E}[\hat{s}^d_{n,i}] = 0$ for all $n \in \mathcal{N}$. Define $S_i^{(N)} = \sum_{n=1}^{N} s^d_{n,i}$, $M_i^{(N)} = \sum_{n=1}^{N} \mathbb{E}[s^d_{n,i}]$, and $\sigma\left(S_i^{(N)}\right)^2 = Var[S_i^{(N)}]$. If, for all i,*

i. *The sequences $\{\hat{s}^d_{1,i}, \hat{s}^d_{2,1}, ...\hat{s}^d_{N,i}\}$ are α-mixing and fulfill the conditions in Lemma 1*

ii. *The coefficients of variation associated with the sequences $\{S_i^{(1)}, S_i^{(2)}, ..., S_i^{(N)}\}$ fulfill condition (ii) of Lemma 2 as $N \to \infty$*

[20] We discuss Lemma 2 further in Supplemental Appendix A.2. Beyond the context in which we apply the Marlow (1967) lemma, it appears to have broad usefulness within economics. For example, a CES aggregator over positive random variables fulfilling the conditions of the lemma should approach lognormality as the lognormal distribution is preserved over exponentiation.

then the distribution of $\frac{M_i^{(N)}}{\sqrt{N}\sigma\left(S_i^{(N)}\right)} \ln\left(\frac{S_i^{(N)}}{M_i^{(N)}}\right)$ *converges in distribution to a lognormal for all* i *as* $N \to \infty$.

The proof follows directly from Lemma 1 and Lemma 2. Lemma 1 allow us to apply an α-mixing central limit theorem to the sum S_i, and Lemma 2 allows us to move to a central limit theorem in logs as all elements of this sum are positive.[21] If the necessary assumptions on $s_{n,i}$ hold, the market access summation S_i converges in distribution to a lognormal as N grows large. We assume S_i is lognormally distributed for some sufficiently large N and as a lognormal raised to a power results in another lognormal distribution each $(S_i)^{\frac{1}{\sigma\gamma_1}}$ will also be lognormally distributed.

3.3 Variation within Place and the Distribution of Fundamentals

We now turn to modelling the distribution of fundamentals, and begin by noting that these are intended to reflect differences in the suitability of a place for habitation or settlement. There is clear evidence for observable geographic attributes, alone and in combination, playing a role in shaping human settlement patterns (Henderson et al. 2018). The substantial differences between areas of high population in terms of many geographic attributes suggests that no one particular observable attribute alone is a sufficient proxy for what makes a location good for human habitation, and that many attributes should contribute to the quality of a place.

We model fundamentals as resulting from random shocks via the geographic attributes of a location, building on the approach of Lee and Li (2013) who similarly model a location's quality as resulting from many random "factors." Using random variation in geography to model locational fundamentals is the cross-sectional analog of random growth models based on Gibrat's law over time, like those of Gabaix (1999a) and Eeckhout (2004), where rather than

[21] Interestingly, an implication of Proposition 1 is that the distribution of S_i should appear normal in both levels and logs. We discuss this further in Section 4 and show that this does indeed hold in Supplemental Appendix D.2.

productivity shocks occurring over time each attribute within a location contributes a productivity or amenity shock to the respective fundamental.

Each location i has many geographic attributes a_{ig}, which are indexed by $g \in \mathcal{G}$, where $\mathcal{G} = \{g \mid g \in \mathbb{N}, 1 \leq g \leq G\}$. Attributes for a productive location could be fertile soil, regular and mild weather patterns, and favorable topography, among many others. We assume all attributes are strictly positive in value and for any g, higher values of a_{ig} reflect *better* realizations of that attribute.[22] We also assume each individual attribute is drawn from a common distribution in all locations, while different attributes may differ in their respective distribution.

For brevity we focus our discussion on productivity fundamentals before returning to consider the similarly constructed amenity fundamentals. The locational productivity fundamental for a location i, denoted A_i, should be a function of its many attributes such that $A_i = F_A(a_{i1}, a_{i2}, ..., a_{iG})$. This function should be increasing in each a_{ig}, to reflect that better attributes increase productivity, such that $\frac{\partial F_A}{\partial a_{ig}} > 0$ for all $g \in \mathcal{G}$. Further, the aggregating function should exhibit complementarities between each of the attributes. That is, the benefit of having reliable rainfall for production is increased when there is better arable land in a location, for instance. This means the aggregating function also needs a positive cross-partial for all arbitrary combinations of attributes, such that $\frac{\partial^2 F_A(\cdot)}{\partial a_{ij} \partial a_{ig}} > 0$, for $j, g \in \mathcal{G}, j \neq g$.

Consistent with these assumptions, we can view the contribution of attributes to the fundamental as representing multiplicative shocks. We assume a Cobb-Douglas form for the aggregating function F_A, consistent with the requirements outlined above. The varying importance of different attributes can

[22] These should not be thought of as being measured in the familiar units for each attribute. Rainfall in inches has a nonlinear relationship with agricultural output, for instance. We instead want a measure reflecting how positive the "shock" from a given attribute is.

be reflected by the exponents $\xi_g > 0$ associated with each g:[23]

$$A_i = \prod_{g \in \mathcal{G}} {a_{ig}}^{\xi_g} \tag{21}$$

Taking the natural log yields the following expression:

$$\ln(A_i) = \sum_{g \in \mathcal{G}} \xi_g \ln a_{ig} \tag{22}$$

where we express the logged fundamental in location i as a sum of random variables $\xi_g \ln a_{ig}$.

It is possible that some attributes a_{ig} are not independent within locations. For example, high July temperatures and the number of growing days may be correlated within places such that knowing the realization of one is informative about the likely values of the other. However, over the large number of attributes of a place there do appear to exist pairs of attributes which appear nearly independent within locations (e.g., topography and rainfall), as we demonstrate in Supplemental Appendix C.4 using data on geographic attributes from Henderson et al. (2018).

Consistent with this we assume that attributes are α-mixing within locations, as in Lee and Li (2013). We define the ordering of the sequence of attributes $\{a_{i1}, a_{i2}, ..., a_{iG}\}$ such that similar attributes are close together (July temperatures and growing days have indices near each other), while independent attributes differ greatly in their index values (rainfall and topography have indices set far apart). Together with further restrictions, given in Lemma 1, on the moments of the random variables $\xi_g \ln a_{ig}$ and the rate of α-mixing, which determines how rapidly the elements of the sequence approach independence, we apply the central limit theorem in Lemma 1 to characterize the distribution of each $\ln A_i$.

[23] We could also include an index for the time t, to allow for attributes a_{igt} to vary over time and to vary in their importance over time ξ_{gt}, which could capture structural transformation of the economy or changing production technologies at time t. In this case, $A_{it} = \prod_{g \in \mathcal{G}} {a_{igt}}^{\xi_{gt}}$ where the fundamentals can vary with t.

Proposition 2: *Define* $\widehat{\xi_g \ln a_{ig}} = \xi_g \ln a_{ig} - \mathbb{E}[\xi_g \ln a_{ig}]$ *for all* $g \in \mathcal{G}$ *and* $i \in \mathcal{N}$*, and define* $\widehat{\ln A_i} = \sum_{g \in \mathcal{G}} \widehat{\xi_g \ln a_{ig}}$ *and* $\sigma\left(\widehat{\ln A_i}\right)^2 = Var[\widehat{\ln A_i}]$ *for all* $i \in \mathcal{N}$*. If the sequences* $\{\widehat{\xi_g \ln a_{ig}}\}$ *are* α*-mixing and fulfill the conditions of Lemma 1 for all* $i \in \mathcal{N}$*, then as* $G \to \infty$*,* $\frac{1}{\sqrt{G}\sigma\left(\widehat{\ln A_i}\right)} \widehat{\ln A_i}$ *converges in distribution to the standard normal distribution for all* $i \in \mathcal{N}$*.*

Proposition 2 follows from Lemma 1. By Proposition 2, as the number of attributes grows large, the log productivity fundamental $\ln A_i$ will converge in distribution to a normal distribution and so A_i will converge in distribution to a lognormal distribution. We assume that, for a large number of attributes, A_i will be lognormally distributed based on this asymptotic argument.

The amenity fundamental is defined similarly, but we allow for different weights as the attributes most relevant for determining quality of life may differ from those influencing productivity. The log of the amenity fundamental, which has weights given by $\iota_g > 0$, is:

$$\ln(U_i) = \sum_{g \in \mathcal{G}} \iota_g \ln a_{ig} \tag{23}$$

and, given the same conditions as on the productivity fundamental, will also converge in distribution to a lognormal as the number of attributes grows large.

We provide support for the appearance of a lognormal distribution for fundamentals in two ways. First, the fundamentals recovered by inverting the model in Allen and Arkolakis (2014), plotted in Supplemental Appendix C.6, appear lognormal for U.S. counties. Second, we use the Henderson et al. (2018) data on attributes and, following our modeling assumptions, calculate a "naive" fundamental by applying our aggregating function.[24] The plots are reported in Supplemental Appendix C.6, and show that aggregating the eleven attributes results in a distribution of fundamentals that appears lognormal. While only suggestive, both the strategy of recovering fundamentals within a

[24]We say the fundamental is "naive" in the sense that we do not know the appropriate weights or scaling of the attributes. The construction of the fundamental is discussed in Supplemental Appendix C.5. A similar exercise was earlier done by Behrens and Robert-Nicoud (2015) for U.S. MSAs.

structural model based on true populations and the construction of a "naive" fundamental from attributes result in strikingly lognormal distributions.

Given lognormally distributed productivity and amenity fundamentals A_i and U_i, we can show that the "own-fundamental" term Ω_i for each location i will be lognormally distributed.

Proposition 3*: If A_i and U_i have a bivariate normal distribution in logs, Ω_i will be lognormally distributed.*

Proposition 3 follows immediately from the properties of lognormals, as either raising a lognormal distribution to a power or multiplying by a positive constant begets another lognormally distributed random variable and multiplying two lognormal random variables which have a bivariate normal distribution in logs also results in another lognormally distributed random variable.

We now consider the spatial distribution of geographic attributes and the implications for the resulting fundamentals, formalizing the discussion in the prior section on the distribution of the exogenous productivity and amenity fundamentals across space. Geographic attributes tend to be correlated across space and nearby locations often have similar topography, rainfall, soil quality, and so on, but as the distance between locations increases the similarity of attributes across locations declines. In Supplemental Appendix C.4 we provide evidence for this pattern of spatial correlations based on the attributes data in Henderson et al. (2018). This pattern of declining similarity with respect to distance is consistent with modeling geographic attributes as being α-mixing with respect to distance.[25]

In our simplified circle geography, we assume that the sequences $\{A_i\}$ and $\{U_i\}$ are α-mixing with respect to distance to reflect the patterns of correlation in geographic attributes across space.[26] This assumption captures the

[25]The concept of α-mixing can be extended to two-dimension spaces, like that of the geographic data, and we provide the definition for α-mixing of random fields in Supplemental Appendix A.3. The complication involves the need to introduce a concept of distance when this information is not directly encoded in the series index. All of our proofs can be generalized to two dimensional geographies, as we show in Supplemental Appendix A.5.

[26]If geographic attributes were independent sequences the α-mixing of $\{A_i\}$ and $\{U_i\}$

potential similarity of nearby locations and how this similarity vanishes with increasing distance, and is consistent with the argument for α-mixing of the elements of the market access summation in the prior section.[27]

3.4 The Distribution of Population

We have now shown that Ω_i and $(S_i)^{\frac{1}{\tilde{\sigma}\gamma_1}}$ are lognormally distributed when realistically modeled to reflect variation in geography and trade costs over space. Using this, we can then show that the population will be lognormally distributed as population in each location i is given by $L_i = \Omega_i(S_i)^{\frac{1}{\tilde{\sigma}\gamma_1}}$. This result is given in Theorem 1.

Theorem 1: *If Ω_i and $S_i^{\frac{1}{\tilde{\sigma}\gamma_1}}$ have a bivariate normal distribution in logs for all $i \in \mathcal{N}$, then L_i follows a lognormal distribution for all $i \in \mathcal{N}$.*

The proof follows directly from the lognormality of Ω_i and $S_i^{\frac{1}{\tilde{\sigma}\gamma_1}}$, and the property that products of lognormal distributions which have a bivariate normal distribution in logs also follow a lognormal distribution.

For the realized population distribution to appear lognormal we further require that populations are not too correlated across locations. While we have proven that the distribution of the population in each i approaches a lognormal, it is possible that the equilibrium population is highly correlated such that the full probability distribution is not realized. We need to demonstrate that the population distribution is also α-mixing, which will ensure that due to the asymptotic independence of the population over space the realized population distribution will reflect the lognormality of the underlying distribution for large N.[28]

would follow directly from Theorem 5.2 of Bradley (2005) and α-mixing of attributes with respect to distance. However, as many attributes are likely not independent, we must assume α-mixing of the fundamentals with respect to distance

[27] We find that the correlation of the constructed "naive" fundamentals across space declines with increasing distance, as shown in in Supplemental Appendix C.6, consistent with the assumption of α-mixing.

[28] The stronger concept of α-mixing implies ergodicity (Frigg et al. 2020). An ergodic process will visit all parts of the probability space associated with the process given large N.

Proposition 4: *If* $\{A_i\}$ *and* $\{U_i\}$ *are* α*-mixing and independent sequences, then* $\{\Omega_i\}$ *is an* α*-mixing sequence.*

The proof follows directly from Theorem 5.2 of Bradley (2005), as α-mixing is maintained over measurable transformations and over combinations of independent α-mixing random sequences.[29] We must make the stronger assumption that A_i and U_i are independent, but given α-mixing of these sequences independence establishes that $\{\Omega_i\}$ will also be α-mixing.[30]

We can then show that the population sequence $\{L_i\}$ will be α-mixing as well, given an additional assumption that the market access terms S_i are also α-mixing. This will ensure that the full probability space of the population distribution will be realized for large N.

Theorem 2: *If* $\{\Omega_i\}$ *and* $\{S_i\}$ *are independent* α*-mixing sequences, then the population sequence* $\{L_i\}$ *is* α*-mixing.*

The proof also follows directly from Theorem 5.2 of Bradley (2005). In Supplemental Appendix A.5 we show that these α-mixing properties and proofs for sequences can be generalized to two-dimensional α-mixing fields and will also hold for more realistic geographies. The α-mixing of the population within the model is consistent with real-world population distributions, as large population centers tend to be surrounded by other populous areas rather than sparsely populated regions.[31] The α-mixing of the population also implies

[29] In Supplemental Appendix A.3 and A.5, we extend Theorem 5.2 of Bradley (2005) from random sequences to random fields in two-dimensional space.

[30] This assumption is necessary for the application of Theorem 5.2 of Bradley (2005) in the proof of Proposition 3, but we will relax this assumption in our simulations and show that it does not appear necessary for the result. Allen and Arkolakis (2014) find a low, but non-zero, correlation of 0.12 between A_i and U_i.

[31] There is a literature on urban shadows which suggests that new cities tend not to form immediately next to existing cities, and which appears to be in tension with the correlation of the population distribution across space. One example of this literature is Bosker and Buringh (2017), which documents a "shadow" surrounding cities in Europe from 800-1800. This shadow is ascribed to forces beyond our model, such as the risk of armed conflict between cities, and results within Bosker and Buringh (2017) still demonstrate a high degree of spatial correlation in the population distribution (see, for example, their Figure 4). Related work on urban *growth* shadows, as in Cuberes et al. (2021) find that

that the very largest cities will not cluster together despite the correlations in population, because the population of different locations will approach independence as distance increases.

4 Results

We now demonstrate that the model successfully generates lognormal population distributions and power law-like city size distributions via simulation. We provide comparative statics based on varying parameter values across simulations to document how changes in congestion, spillovers, and trade costs influence the observed power law. We identify changes to the power law in the directions implied by the empirical literature. Finally, we show that Gibrat's law holds within the model when the aggregate population increases, showing that size-invariant growth is a feature of a lognormal equilibrium population distribution based on variation in geography and trade, in contrast to earlier literature that took random growth to be the basis for lognormal populations.

4.1 Simulation of the Population Distribution

We first simulate the model to demonstrate that the resulting populations are indeed lognormally distributed and that the city size distribution appears to follow a power law. We simulate the results within a two dimensional geography. Each location in the model is a place that can host a settlement.[32] Note that the definition of a "location" is not specified by the model, beyond being a place within which local spillovers occur, and these could either be large regions or small locales.[33] We define the most populous 5% of locations

the growth of peripheral regions near large urban centers is influenced by the central city, with locations near urban centers tending to grow faster over the past century, which is also consistent with spatial correlation in populations.

[32]This interpretation matches that in Redding and Rossi-Hansberg (2017), which frames locations as regions which can potentially hold a single settlement.

[33]That the model is ambiguous on the level of aggregation of population means it is consistent with the observation of the characteristic population distribution at varying levels of aggregation, as in Holmes (2010), Rozenfeld et al. (2011), and Mori et al. (2020). Spillovers are unlikely to be purely local at any level of aggregation, and so differing levels of ag-

as "cities" within the model, to demonstrate that the tail behavior of the resulting population distribution mirrors the appearance of a power law in empirical city size distributions. To ensure dispersion in trade costs while remaining consistent with the triangle inequality and maintaining symmetry, we model settlements as occurring randomly over a large surface and take the Euclidean distance between all settlements.[34] We simulate a large geography and take the central locations as the geography of interest to limit the impact of border effects on the population distribution. We are left with a central geography consisting of approximately 20,000 settlements.[35]

We take model parameters from the literature and from Allen and Arkolakis (2014) where possible. We first create randomly-generated draws of exogenous productivity and amenity fundamentals with declining spatial correlation. Fundamentals are drawn from lognormal distributions with parameters $\sigma_{LN} = 1$ and $\mu_{LN} = 0$, and we induce spatial correlation in the fundamentals using a Choleski decomposition.[36] We allow the productivity and amenity fundamentals in a location to be correlated and set the correlation between A_i and U_i within each location i to $\rho_{AU} = 0.12$ to match the correlation between the recovered productivity and amenity fundamentals in Allen and Arkolakis (2014).

The magnitude of local productivity spillovers is given by $\alpha = 0.03$, in line with the estimates in Combes et al. (2008) and those surveyed in Rosenthal and Strange (2004) and Combes and Gobillon (2015).The model contains an

gregation may require different parameters governing "local" spillovers that are a useful abstraction from more complex patterns of spillovers.

[34]An example of a portion of this "dartboard" geography can be seen in Supplemental Appendix D.1. We could alternatively model trade costs as having an idiosyncratic component to ensure dispersion, and not respect the triangle inequality or symmetry. We choose the more restrictive setting without an idiosyncratic component for our main results to demonstrate that only a limited degree of dispersion is necessary. We simulate with additional idiosyncratic shocks to trade costs in Supplemental Appendix D.4.

[35]We uniformly distribute 30,000 settlements across a 1200-by-1200 grid and discard those within 100 cells of a border. This leaves an expected number of settlements of $\frac{100}{144} * 30000 = 20,833.\bar{3}$. We draw new randomly drawn fundamentals each simulation.

[36]We assume the degree of spatial correlation of the log-scale fundamental declines exponentially, consistent with the empirical attribute correlations we show in Supplemental Appendix C.6, so that $\rho_{ij} = e^{-\delta_\rho d_{ij}}$. For $j = i$, this gives $\rho_{ii} = 1$ as $d_{ii} = 0$. We set $\delta_\rho = 0.5$.

isomorphism which we use to parameterize congestion costs. As discussed in Allen and Arkolakis (2014), the model is isomorphic to one with a fixed quantity of housing where spending on housing is δ and $\beta = -\frac{\delta}{1-\delta}$. Congestion costs are parameterized to match a level of spending on housing of 25% of income, which gives a congestion parameter of $\beta = -\frac{1}{3}$, consistent with the estimates in Combes et al. (2019) and Davis and Ortalo-Magné (2011). We model trade costs as an exponential function of distance, $\tau_{ij} = e^{\delta_{TC} d_{ij}}$ and set $\delta_{TC} = 0.001$.[37] We vary these parameters in Supplemental Appendix D.3. We set the elasticity of substitution $\sigma = 5$, as in Redding and Rossi-Hansberg (2017) and consistent with the estimates in Simonovska and Waugh (2014).

Figure IV shows the equilibrium population distribution associated with a random draw of productivity and amenity fundamentals and trade costs.[38] The log of the population distribution very closely matches the overlaid normal distribution, demonstrating lognormality. The upper-right panel shows a quantile-quantile (QQ) plot of the log population and a normal distribution, demonstrating very close fit throughout the full distribution. The output in the upper panels is very similar to Figure II for the full U.S. population distribution. Given the lognormality of the population distributions, the most populated locations in our model will appear to follow a power law distribution as demonstrated in Section 2. Concentrating only on the most populated 5% of locations, in the bottom panel of Figure IV we find the model generates power law-like city size population distributions like those commonly identified in the data. Indeed, this panel is similar to Figure I for U.S. cities and the log rank-size regression on this simulated data gives a slope of -0.977, close to the classic Zipf's Law result of a slope of -1 for this particular random draw of fundamentals.

[37] Allen and Arkolakis (2014) estimate a value of $\delta = 0.56$ for road travel when the width of the continental U.S. is normalized to 1, given an elasticity parameter of $\sigma = 9$. The geography we simulate has a width of 1000 and we use $\sigma = 5$. The difference in the normalized distance and the necessary re-scaling due to changing the elasticity of substitution imply a scaled parameter of 0.00112, near the value we choose.

[38] Whenever we present a single random draw, we present the first draw using our seed value. Our seed value is the four-digit catalog number of Columbia Economics Professor Serena Ng's graduate macroeconometrics course.

Figure IV:
Example of the Equilibrium Population Distribution

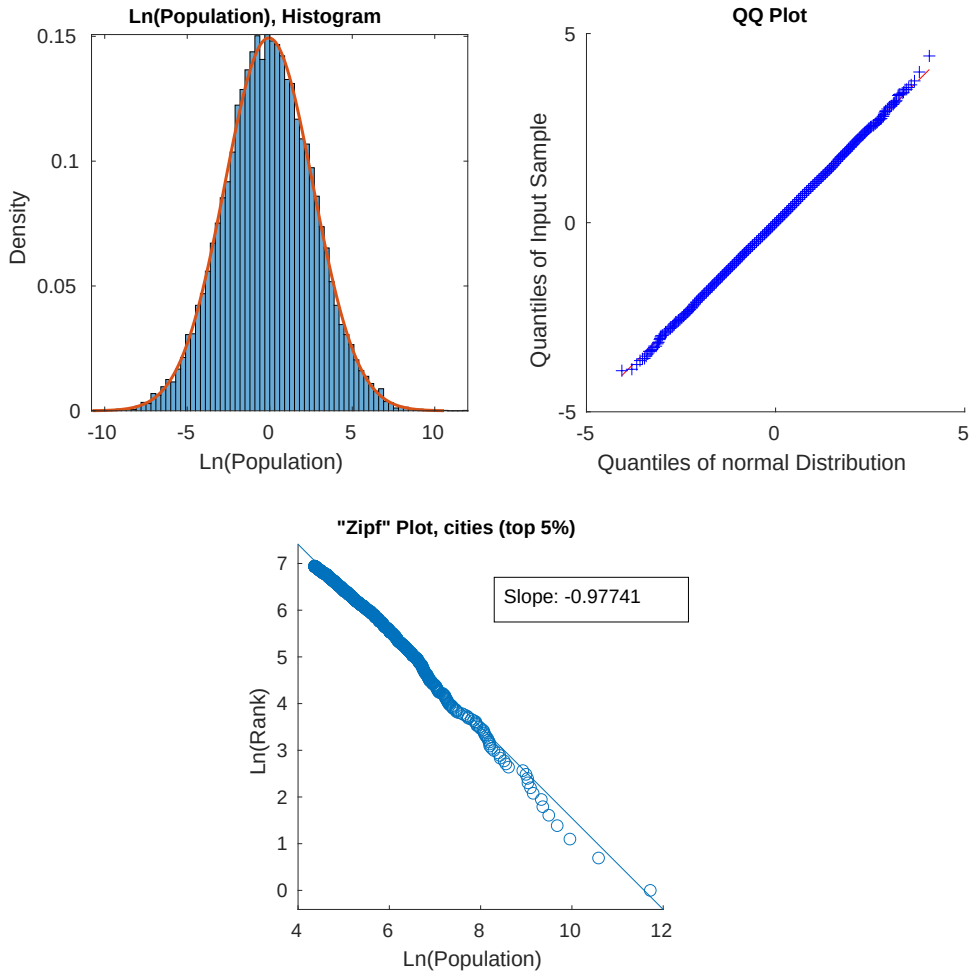

Notes: The top left panel shows the model's log population appears to follow a normal distribution. The top right panel contains a QQ plot of the model's log population distribution, indicating that it very closely matches a normal distribution. The log rank-size plot at the bottom shows a strong resemblance to the typical log rank-size plot for cities along with the characteristic divergence of the largest locations below the trendline.

Figure V:
Smoothed Output Over 1000 Simulations

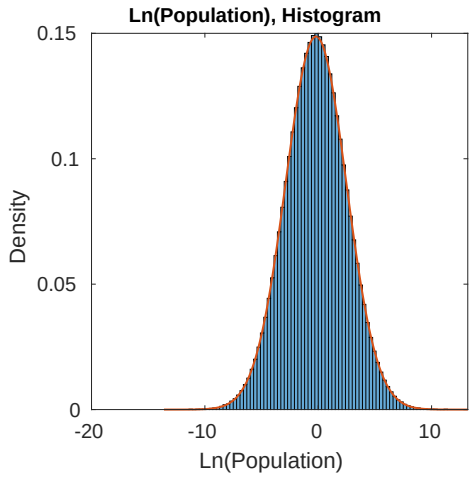

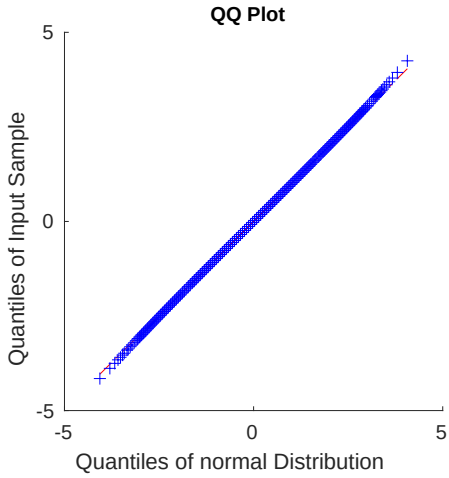

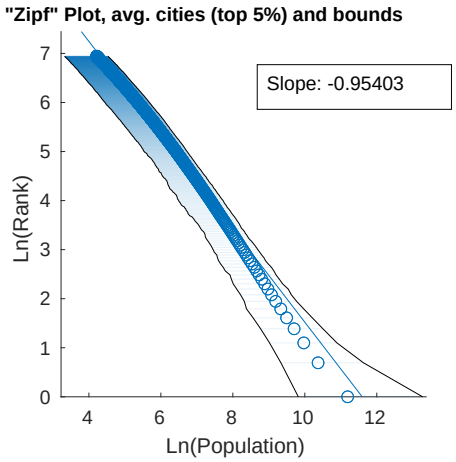

1000-draw MC	Value
Coef. of Avg.	-.954
Avg. over Coefs	-.952
Std. Dev.	(.033)
Min	-1.052
5pct	-1.007
25pct	-.976
50pct	-.952
75pct	-.931
95pct	-.895
Max	-.855

Notes: The smoothed population distribution resulting from 1000 simulations of model is in the upper left panel, and the resulting QQ plot is on the upper right. Both show that the equilibrium population distribution appears lognormal. The city size distributions from the 1000 simulations are in the lower left, and statistics over model simulations the lower right. The slope on the lower left represents the slope taken over the average of log(pop) at each rank over 1000 simulations, and the bounds contain 95% of the log populations at each rank of the distribution. The table displays statistics over the 1000 estimated power law coefficients from the simulations.

In Supplemental Appendix D.2, we also check that the summation term S_i behaves as predicted by Proposition 1 and the conditions in Theorem 2 which imply that this term should appear normal in both levels and logs and be independent from the own-lognormal term for each location. We find evidence that both of these hold predictions within our simulations. When we induce further idiosyncratic variation in trade costs in Supplemental Appendix D.4 the fit of S_i to the normal distribution in both levels and in logs improves, consistent with the importance of dispersion in trade costs for the distribution of market access.

We next demonstrate the robustness of the lognormal population distribution by performing 1000 simulations, each time drawing a new randomly generated distribution of fundamentals. Figure V displays smoothed results over 1000 simulations of the model.[39] The QQ plot also demonstrates lognormality of the expected log population over these simulations. We verify the robustness of the power law coefficient estimate across the simulations, with an average coefficient across the 1000 simulations of -0.95, with a standard deviation of 0.03. 90% of estimated coefficients are between -0.900 and -1.004. Performing the (log) rank-size regression on the smoothed distribution delivers a slope of -0.95. The parameter values used here are consistent with the literature and estimates are near the Zipf's Law of -1 for all simulated values. While the model using standard parameters from the literature closely approximates the Zipf's Law coefficient of -1, we maintain our argument that the -1 coefficient is not a meaningful feature of the data. Changes in scale and the truncation point can influence the estimate, as discussed in Section 2 and Supplemental Appendix B. Nonetheless, it is interesting to note that the estimated power law exponent appears consistent with Zipf's Law for typical parameter values in the literature.

We test each of the 1000 simulated population distributions against the null hypothesis that the logged population distribution is normally distributed using the Kolmogorov-Smirnov, Lilliefors, and Jarque-Bera tests. The results

[39]The log of population is averaged at each rank of the distribution over the 1000 simulations. Results are similar when averaging the population and taking the log.

Table I: Normality Tests

	Kolmogorov-Smirnov	Lilliefors	Jarque-Bera
Rejected at 1%	0.000	0.022	0.171
Rejected at 5%	0.001	0.103	0.353

Notes: Table shows the share of tests for a normal distribution rejected for the log equilibrium population of 1000 simulations.

of these tests are given in Table I. None of the tests reliably reject the normal distribution for the logged population. Rejections of normality occur most often under the Jarque-Bera test, which tests for skewness and kurtosis.[40] A degree of kurtosis is evident in the QQ plot as both tails appear slightly heavier than a normal distribution, which may be attributable to the finite grid.

4.2 Comparative Statics Across Simulations

We next simulate the comparative statics of the estimated power law coefficient for the city size distribution, testing its sensitivity to changes in model parameters. Changing parameters alters the estimated coefficient of the log rank-size regression, which we denote θ_1 as in Equation 1. We perform 100 simulations for each of 150 combination of parameters.[41] A summary of the signs of changes (estimated by a regression given in Supplemental Appendix D.3) is provided in Table II.

The comparative statics of our model demonstrate changes in the estimated power law coefficient in line with the empirical evidence. Increasing the benefits of agglomeration by raising $\alpha > 0$ results in a more unequal city size distribution (greater dispersion, or a flatter slope) and increasing local congestion costs by reducing $\beta < 0$ results in a more equal distribution (less

[40]The higher rejections under the Jarque-Bera test may also be attributable to the inappropriateness of this test for spatial data, similar to its inappropriateness for time series data documented in Bai and Ng (2005).

[41]We simulate for 5 values of α, 6 values of β, and 5 values of δ_{TC} given in Supplemental Appendix D.3. The geography has the same dimensions as our baseline simulations but we change the number of locations in the full geography to 10000 to reduce computation time.

Table II: Comparative Statics

	$\frac{\partial \theta_1}{\partial \alpha}$	$\frac{\partial \theta_1}{\partial \beta}$	$\frac{\partial \theta_1}{\partial \delta_{TC}}$
Sign of change	+	+	+

Notes: Direction of the change in slope coefficient in the (log) rank-size regression for changes in α, β, and δ_{TC}, holding other parameters constant. "+" means the estimated slope (which is negative by construction) has become flatter. This implies that the largest large cities are relatively bigger. Note that $\beta < 0$, so an increase in β means a decrease in congestion. The signs are from a regression of the parameters on the estimated coefficients (discussed in Supplemental Appendix D.3)

dispersion, or a steeper slope). Increasing trade costs by increasing the rate at which these costs grow with distance, $\delta_{TC} > 0$, likewise results in a more unequal city size distribution. In many developing countries, the city size distributions are highly unequal, generating the flatter slopes in the log-log regression documented in Duben and Krause (2021). These unequal city size distributions be attributable to high domestic transportation costs, which are often substantially higher in developing than in developed countries. Atkin and Donaldson (2015) estimate that domestic trade costs are roughly four to five times higher in Nigeria and Ethiopia than in the U.S., in line with the empirical evidence documented in Teravaninthorn and Gaël (2009). These high domestic trade costs could contribute to the phenomenon of very large metropolises relative to secondary cities ("primate cities") within the developing world. Additionally, the flattening slope in the U.S. in recent decades, documented in Gabaix and Ioannides (2004), could be a result of increased agglomeration benefits in the modern services economy.

4.3 Gibrat's Law

Allen and Arkolakis (2014) demonstrate that the population vector is scaled by changes in the aggregate population, but the relative populations over locations are not changed by changes in the total population. We now demonstrate

that based on this property the equilibrium population distribution demonstrates proportional growth and satisfies Gibrat's law in response to increases in the aggregate population $\bar{L}$. We can write Equation 31, the matrix form representation of Equation 19 as:

$$\tilde{\mathbf{h}} = \mathbf{J}[\tilde{\mathbf{h}}]^{\frac{\gamma_2}{\gamma_1}}$$

where $\tilde{h}_{i'} = h_{i'}\bar{W}^{\frac{\sigma-1}{1-\frac{\gamma_2}{\gamma_1}}}$, the notation $[\cdot]^a$ indicates raising each element of the vector to the power a, and the matrix $\mathbf{J}$ is given in Supplemental Appendix A.4. As this relationship must hold for any level of $\bar{L}$, changing $\bar{L}$ does not impact the resulting population distribution even as it impacts welfare ($\bar{W}$, which is the same across all locations). That is, a percentage increase in overall population will result in each location experiencing population growth of the same percentage. As a result, population growth rates will be unrelated to initial population and Gibrat's law will hold within the equilibrium of this model.

This is a key difference between our explanation for observed population distributions based on locational fundamentals and trade and the prior literature on random growth models. Rather than being the force creating the equilibrium distribution, random growth is a feature of an equilibrium based on the underlying characteristics of place and trade. This view is supported by the absence of Gibrat's law in systems that are in transition or have suffered dis-equilibrating shocks (Desmet and Rappaport 2017; Davis and Weinstein 2002, 2008).

5 Conclusion

The power law-like distribution of city populations is a striking empirical regularity that holds across countries and over millennia. In this paper, we demonstrate that a broad class of economic geography models generate these characteristic population distributions when modeled with a realistic geography. We integrate insights from economic geography theory regarding the importance

of both the qualities of a location and its market access for its population into the extensive literature on power law-like population distributions and Zipf's Law. Viewing population distributions as arising naturally in response to favorable geography and trade access provides a simple explanation for the emergence of the distinctive city size distribution. This explanation is consistent with the persistence of human settlements, the recovery of cities from disasters, and the random growth of cities in equilibrium.

References

Adão, R., A. Costinot, and D. Donaldson (2023). Putting Quantitative Models to the Test: An Application to Trump's Trade War. Technical report, National Bureau of Economic Research.

Alix-Garcia, J. and E. A. Sellars (2020). Locational fundamentals, trade, and the changing urban landscape of mexico. *Journal of Urban Economics 116*, 103213.

Allen, T. and C. Arkolakis (2014). Trade and the Topography of the Spatial Economy. *Quarterly Journal of Economics 129*(3), 1085–1140.

Atkin, D. and D. Donaldson (2015). Who is Getting Globalized? The Size and Implications of Intranational Trade Costs. Working paper.

Auerbach, F. (1913). Das Gesetz der Bevölkerungskonzentration. *Petermann's Geographische Mitteilungen*.

Auerbach, F. and A. Ciccone (2023). The Law of Population Concentration. *Envmt. and Planning B: Urban Analytics and City Sc. 50*(2), 290–298.

Bai, J. and S. Ng (2005). Tests for Skewness, Kurtosis, and Normality for Time Series Data. *Journal of Business and Economic Statistics 23*(1), 49–60.

Behrens, K. and F. Robert-Nicoud (2015). Agglomeration Theory with Heterogenous Agents. *Handbook in Regional and Urban Economics Ch. 5*.

Blank, A. and S. Solomon (2000). Power laws in cities population, financial markets and internet sites (scaling in systems with a variable number of components). *Physica A: Statistical Mechanics and its Applications 287*(1), 279–288.

Bosker, M. and E. Buringh (2017). City seeds: Geography and the origins of the european city system. *Journal of Urban Economics 98*, 139–157.

Bradley, R. C. (2005). Basic Properties of Strong Mixing Conditions. A Survey and Some Open Questions. *Probability Surveys 2*(N.A.).

Brakman, S., H. Garretsen, and M. Schramm (2004). The strategic bombing of German cities during World War II and its impact on city growth. *Journal of Economic Geography 4*(2), 201–218.

Brakman, S., H. Garretsen, C. Van Marrewijk, and M. Van Den Berg (1999). The Return of Zipf: Towards a Further Understanding of the Rank-Size Distribution. *Journal of Regional Science 39*(1), 183–213.

Combes, P.-P., G. Duranton, and L. Gobillon (2008). Spatial wage disparities: Sorting matters! *Journal of Urban Economics 63*(2), 723–742.

Combes, P.-P., G. Duranton, and L. Gobillon (2019). The Costs of Agglomeration: House and Land Prices in French Cities . *Review of Economic Studies*, 1556–1589.

Combes, P.-P. and L. Gobillon (2015). Chapter 5 - The Empirics of Agglomer-

ation Economies. In *Handbook of Regional and Urban Economics*, Volume 5, pp. 247–348. Elsevier.

Cuberes, D., K. Desmet, and J. Rappaport (2021). Urban growth shadows. *Journal of Urban Economics 123*, 103334.

Córdoba, J.-C. (2008). On the distribution of city sizes. *Journal of Urban Economics 63*(1), 177–197.

Davis, D. R. and D. E. Weinstein (2002). Bones, Bombs, and Break Points: The Geography of Economic Activity . *American Economic Review 92*(5), 1269–1289.

Davis, D. R. and D. E. Weinstein (2008). A Search for Multiple Equilibria in Urban Industrial Structure. *Journal of Regional Science 48*(1), 29–65.

Davis, M. A. and F. Ortalo-Magné (2011). Household expenditures, wages, rents. *Review of Economic Dynamics 14*(2), 248–261.

Desmet, K. and J. Rappaport (2017). The settlement of the United States, 1800–2000: The long transition towards Gibrat's law. *Journal of Urban Economics 98*, 50–68.

Duben, C. and M. Krause (2021). Population, light, and the size distribution of cities. *Journal of Regional Science*, 189–211.

Eeckhout, J. (2004). Gibrat's Law for (All) Cities. *American Economic Review*, 1429–1451.

Eeckhout, J. (2009). Gibrat's Law for (All) Cities: Reply. *American Economic Review 99*(4), 1676–83.

Frigg, R., J. Berkovitz, and F. Kronz (2020). The Ergodic Hierarchy. In E. N. Zalta (Ed.), *The Stanford Encyclopedia of Philosophy* (Fall 2020 ed.). Metaphysics Research Lab, Stanford University.

Fujita, M., P. Krugman, and A. J. Venables (1999, 06). *The Spatial Economy: Cities, Regions, and International Trade*. The MIT Press.

Gabaix, X. (1999a). Zipf's Law and the Growth of Cities. *The American Economic Review 89*(2), 129–132.

Gabaix, X. (1999b). Zipf's Law for Cities: An Explanation. *The Quarterly Journal of Economics*.

Gabaix, X. (2009). Power Laws in Economics and Finance. *Annual Review of Economics 1*(1), 255–294.

Gabaix, X. and Y. M. Ioannides (2004). The Evolution of City Size Distributions. *In: Handbook of Regional and Urban Economics*, 2341–2378.

Gibrat, R. (1931). *Les inégalités économiques.* Paris: Librairie du Recueil Sirey.

Helpman, E. (1998). The Size of Regions. *Topics in Public Economics: Theoretical and Applied Analysis*, 33–54.

Henderson, J. V., T. Squires, A. Storeygard, and D. Weil (2018). The Global

Distribution of Economic Activity: Nature, History, and the Role of Trade. *The Quarterly Journal of Economics 133*(1), 357–406.

Herrndorf, N. (1984). A Functional Central Limit Theorem for Weakly Dependent Sequences of Random Variables. *The Annals of Probability 12*(1), 141 – 153.

Holmes, Thomas J. andLee, S. (2010). Cities as Six-by-six-mile Squares: Zipf's Law? In *Agglomeration Economics*. NBER.

Johnson, N., R. Jedwab, and M. Koyama (2019). Pandemics, Places, and Populations: Evidence from the Black Death. *Working Paper*.

Krugman, P. (1991). Increasing returns and economic geography. *Journal of Political Economy 99*(3), 483–499.

Krugman, P. (1996). *The Self-Organizing Economy*. Blackwell.

Lee, S. and Q. Li (2013). Uneven landscapes and city size distributions. *Journal of Urban Economics 78*, 19–29.

Malevergne, Y., V. Pisarenko, and D. Sornette (2011). Gibrat's Law for Cities: Uniformly Most Powerful Unbiased Test of the Pareto Against the Lognormal. *Physical Review*.

Marlow, N. (1967). A Normal Limit Theorem for Power Sums of Independent Random Variables. *Bell System Technical Journal 46*(9), 2081–2089.

Mori, T., T. E. Smith, and W.-T. Hsu (2020). Common power laws for cities and spatial fractal structures. *Proceedings of the National Academy of Sciences 117*(12), 6469–6475.

Nordhaus, W. D. (2006). Geography and macroeconomics: New data and new findings. *Proceedings of the Natl Academy of Sciences 103*(10), 3510–3517.

Nunn, N. and D. Puga (2012). Ruggedness: The Blessing of Bad Geography in Africa. *Review of Economics and Statistics 94*(1), 20–36.

Rante, R., F. Trionfetti, and P. Verma (2024, March). The Size Distribution of Cities: Evidence from the Lab. working paper or preprint.

Rappaport, J. and J. D. Sachs (2003). The United States as a Coastal Nation. *Journal of Economic Growth 8*(1), 5–46.

Redding, S. J. (2016). Goods trade, factor mobility and welfare. *Journal of International Economics*.

Redding, S. J. and E. Rossi-Hansberg (2017). Quantitative Spatial Economics. *Annual Review of Economics*.

Rosenthal, S. S. and W. C. Strange (2004). Chapter 49 - Evidence on the Nature and Sources of Agglomeration Economies. In J. V. Henderson and J.-F. Thisse (Eds.), *Cities and Geography*, Volume 4 of *Handbook of Regional and Urban Economics*, pp. 2119–2171. Elsevier.

Rossi-Hansberg, E. and M. Wright (2007). Urban Structure and Growth. *The Review of Economic Studies*, 597–624.

Rozenfeld, H. D., D. Rybski, X. Gabaix, and H. A. Makse (2011). The Area and Population of Cities: New Insights from a Different Perspective on Cities. *American Economic Review 101*(5), 2205–25.

Simonovska, I. and M. E. Waugh (2014). The elasticity of trade: Estimates and evidence. *Journal of International Economics 92*(1), 34–50.

Teravaninthorn, S. and R. Gaël (2009). Transport Prices and Costs in Africa: A Review of the Main International Corridors. *World Bank Report*.

Tobler, W. (1970). A Computer Movie Simulating Urban Growth in the Detroit Region. *Economic Geography 46*.

Zipf, G. K. (1949). Human Behavior and the Principle of Least Effort. *Addison-Wesley Press*.

SUPPLEMENTAL APPENDIX

for "Populations in Spatial Equilibrium"

Matthew Easton and Patrick W. Farrell

A Discussion of Main Text Results and Proofs

A.1 Algebra for "Pareto Form" of Lognormal PDF

The density function of a lognormal distribution is given by:

$$f(x) = \frac{1}{x\sigma\sqrt{2\pi}} \exp\left(-\frac{(\ln(x)-\mu)^2}{2\sigma^2}\right)$$

Expanding the square and grouping the $ln(x)$ terms yields:

$$f(x) = \frac{1}{x\sigma\sqrt{2\pi}} \exp\left(\ln\left(x^{\left(\frac{-\ln(x)+2\mu}{2\sigma^2}\right)}\right) - \frac{\mu^2}{2\sigma^2}\right)$$

Applying $e^{\ln(a^b)} = a^b$ and combining with x^{-1}:

$$f(x) = \frac{1}{\sigma\sqrt{2\pi}} \exp\left(-\frac{\mu^2}{2\sigma^2}\right) x^{-\left(\frac{\ln(x)-2\mu}{2\sigma^2}\right)-1}$$

Writing the constant term $\frac{1}{\sigma\sqrt{2\pi}}$ as Γ, the lognormal distribution can be written as:

$$f(x) = \Gamma x^{-\alpha(x)-1} \quad \text{, where } \alpha(x) = \frac{\ln(x)-2\mu}{2\sigma^2}$$

which is the same as Equation 3 in the main text. The representation of the lognormal PDF here appears in Malevergne et al. (2011), and is similar to that in Eeckhout (2009).

A.2 Discussion of Lemma 2 (Marlow 1967)

A demonstration of the apparent normality in both levels and logs of sum of positive random variables is included in the main text in Figure A.I, which shows the sums of lognormal ($\exp(N(0,1))$, truncated normal (a standard normal truncated at 0), and (0,1] uniform random variables. The sums of these random variables converge to normal distributions, while the log of the sum also appears to follow a normal distribution.

Examples of sums over several positive random variables (lognormal, truncated normal, and uniform) are presented in Figure A.I, exhibiting the appearance of normality in both levels and logs for these sums.

The Marlow result is interesting, as it appears to imply that a sum of positive random variables can be viewed as approaching a lognormal or normal distribution for large N. However, if we are considering both the normal and lognormal approximations for a sum of positive random variables we can demonstrate convergence of the lognormal approximation to the equivalent normal approximation—that is, the lognormal and normal approximation will be identical in the limit. The following discussion draws on Mazmanyan et al. (2008).

For simplicity, consider an approximation of $i.i.d$ positive random variables with mean m and variance s^2. The normal approximation will have parameters $\mu_N = nm = M$ and $\sigma_N^2 = ns^2$. We will now define the parameters for the lognormal approximation of the sum.

First, define the coefficient of variation as

$$C_v = \frac{\sqrt{ns^2}}{nm} = \frac{\sqrt{n}s}{nm} \tag{24}$$

As n grows large, $C_v \to 0$.

The parameters μ_X and σ_X of the lognormal approximation can be found by

$$\sigma_X^2 = \ln(1 + C_v^2) \tag{25}$$

Figure A.I:
Sums of Positive Random Variables Drawn from Various Distributions

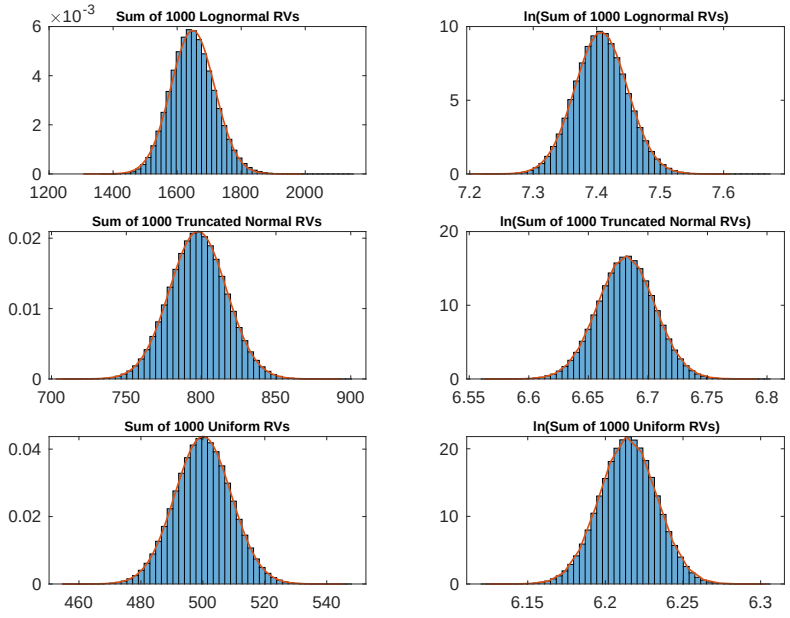

Notes: Histograms show 1,000,000 replications. The random variables in the first row are drawn from a lognormal distribution with parameters $\mu_{LN} = 0, \sigma_{LN} = 1$, the middle row from a truncated normal distribution with parameters $\mu_{TN}, \sigma_{TN} = 0$ and minimum value $\alpha = 0.001$, and the bottom row from a uniform distribution on $(0, 1]$. The red overlaid line represents a normal distribution with the same mean and standard deviation as the underlying sums in each panel. The sums appear distributed normally in both levels (column 1) and in logs (column 2), as implied by Lemma 1.

$$\mu_X = \ln(nm) - \frac{\sigma_X^2}{2} \tag{26}$$

As $C_v \to 0$ when $n \to \infty$, Equation (25) gives that as $n \to \infty$:

$$\sigma_X^2 \to C_v^2 \quad \text{, so} \quad \sigma_X \to C_v \quad \text{, and } \sigma_X \to 0 \tag{27}$$

Now we demonstrate that the lognormal approximation converges to the expected normal. As, for some m, $P(||x - M|| > \epsilon | n \geq m) = 0$, so $\frac{x}{M} \to_{a.s.} 1$. We can write $\frac{x}{M} \cdot \sigma_X \to \frac{\sqrt{n}s}{nm}$, and so $x\sigma_X \to \sqrt{n}s = \sigma_N$. This means $\frac{1}{x\sigma_X\sqrt{2\pi}} \to$

$\frac{1}{\sigma_N\sqrt{2\pi}}$.

Similarly, $x = \frac{xM}{M}$, so $\ln(x) = \ln(M) + \ln(\frac{x}{M})$. As $\frac{x}{M} \to 1$, so $\ln(\frac{x}{M}) \to \frac{x-M}{M}$. As $\mu_X = \ln(M) - \frac{\sigma_X^2}{2}$, and $\sigma_X \to C_v \to 0$, and $M = \mu_N$ then we have

$$\frac{\ln(x) - \mu_x}{\sigma_X} \to \frac{\ln(M) + (\frac{x-M}{M}) - \ln(M)}{\sigma_X} = \frac{x-M}{M\sigma_X} \to \frac{x-M}{M \cdot C_v} = \frac{x-\mu_X}{\sigma_N} \quad (28)$$

So we have shown, as $n \to \infty$,

$$f(x) = \frac{1}{x\sigma_X\sqrt{2\pi}} e^{-\frac{1}{2}\left(\frac{\ln(x)-\mu_X}{\sigma_X}\right)^2} \to \frac{1}{\sigma_N\sqrt{2\pi}} e^{-\frac{1}{2}\left(\frac{x-\mu_N}{\sigma_N}\right)^2} \quad (29)$$

So as n increases, the lognormal approximation to the sum approaches the normal approximation.

A.3 Definitions of α-mixing, sequences and fields

Definition 1,* α*-mixing (sequences): *Suppose* $X := (X_k, k \in \mathbb{Z})$ *is a (not necessarily stationary) sequence of random variables. For* $-\infty \leq J \leq L \leq \infty$*, define the* σ*-field*

$$\mathcal{F}_J^L := \sigma\left(X_k, J \leq k \leq L(|k \in \mathbb{Z}\right).$$

The notation $\sigma(\ldots)$ *means the* σ*-field* $\subset \mathcal{F}$ *generated by* $(\ldots)$*. Define:*

$$\alpha\left(\mathcal{F}_{-\infty}^{j}, \mathcal{F}_{j+n}^{\infty}\right) = \sup_{A \in \mathcal{F}_{-\infty}^{J}, B \in \mathcal{F}_{j+n}^{\infty}} |\mathbb{P}(A \cap B) - \mathbb{P}(A)\mathbb{P}(B)|.$$

For each $n \geq 1$*, define:*

$$\alpha(n) := \sup_{j \in \mathbb{Z}} \alpha\left(\mathcal{F}_{-\infty}^{j}, \mathcal{F}_{j+n}^{\infty}\right),$$

The random sequence X *is said to be "strongly mixing" (or " α-mixing") if* $\alpha(n) \to 0$ *as* $n \to \infty$*.*

The definition above is drawn from Section 2.1 of Bradley (2005), which includes further discussion and the definitions of additional mixing conditions.[42] The ordering of the random variables X_k, in this definition, reflects the time-series nature of this formulation and reflects the "time" of the realization. We instead order the attribute type indices $g \in \mathcal{G}$ in terms of the similarity of the attributes, such that the difference in index reflects the "distance" between attributes $g, g' \in \mathcal{G}$.

The following definition of α-mixing for random fields is used in the more general version of our proofs for a two-dimensional geography in the Supplemental Appendix, rather than the simpler "linear" geography presented in the main text.

Definition 2,* α*-mixing (fields): *Suppose* $\{X_i\}, i \in \mathbb{Z}^2$ *is a stationary random field where each* X_i *is drawn from a common distribution. For disjoint*

[42] For additional discussion, see Billingsley (1995).

sets S, T, define the σ-fields:

$$\mathcal{F}_S := \sigma\left(X_s, s \in S)\right), \mathcal{F}_T := \sigma\left(X_t, t \in T)\right).$$

The notation $\sigma(\ldots)$ means the σ-field $\subset \mathcal{F}$ generated by $(\ldots)$. Define:

$$\alpha\left(S, T\right) = \sup_{A \in \mathcal{F}_S, B \in \mathcal{F}_T} |\mathbb{P}(A \cap B) - \mathbb{P}(A)\mathbb{P}(B)|.$$

Define $dist(S, T) = \inf_{s \in S, t \in T} \|s - t\|$, where $\|\cdot\|$ denotes the Euclidean norm. For each $k \geq 1$ and $u, v \in \mathbb{R}_{++}$, define:

$$\alpha(k; u, v) := \sup_{S,T} \alpha\left(S, T\right),$$

where the supremum is taken over all disjoint subsets S, T with $|S| \leq u, |T| \leq v$ such that $dist(S, T) \geq k$. The random field $\{X_i\}$ is said to be "strongly mixing" (or "α-mixing") if $\alpha(k; \infty, \infty) \to 0$ as $k \to \infty$.

The definition above is drawn from Doukhan (1994) and Bradley (1993), both of which also include further discussion and additional mixing concepts for fields. The key distinction from the definition for sequences introduced earlier is the need to incorporate a concept of distance, which previously was summarized by the indices when considering α-mixing of a sequence.

A.4 Population as a random variable

The system of equations describing the population distribution, given for a particular location i in Equation 19 can be expressed in matrix form as:

$$\theta \mathbf{h} = \mathbf{J}[\mathbf{h}]^{\frac{\gamma_2}{\gamma_1}} \tag{30}$$

where $\theta = \bar{W}^{\sigma-1}$, each element of the vector $\mathbf{h}$ is given by $h_i = L_i^{\tilde{\sigma}\gamma_1}$, and $[\mathbf{h}]^{\frac{\gamma_2}{\gamma_1}}$ indicates raising each element of the vector $\mathbf{h}$ to the power $\frac{\gamma_2}{\gamma_1}$. The matrix $\mathbf{J}$, where elements $j_{i,n} = A_i^{\tilde{\sigma}(\sigma-1)} U_i^{\tilde{\sigma}\sigma} \tau_{i,n}^{1-\sigma} A_n^{\tilde{\sigma}\sigma} U_n^{\tilde{\sigma}(\sigma-1)}$, is given by

$$J = \begin{bmatrix} j_{1,1} & j_{1,2} & \cdots & j_{1,N} \\ j_{2,1} & j_{2,2} & \cdots & j_{2,N} \\ \cdots & \cdots & \cdots & \cdots \\ j_{N,1} & j_{N,2} & \cdots & j_{N,N} \end{bmatrix}$$

where $\mathbf{J}$ is an $\bar{N} \times \bar{N}$ random matrix, with its elements consisting of the realizations for fundamentals and trade costs for all locations. The vector $\mathbf{h}$, which consists of transformations of the population vector, is the eigenvector corresponding to the leading eigenvalue of this random matrix as shown in the online appendix to Allen and Arkolakis (2014). The eigenvectors of random matrices are themselves random vectors, which motivates our treatment of each L_i as a random variable.[43]

Note that each sequence $s_{n,i}$ for each i can be written as the vector $\mathbf{s}_i$ resulting from the following matrix multiplication:

$$\mathbf{s}_i = \mathbf{K}[\mathbf{h}]^{\frac{\gamma_2}{\gamma_1}} \tag{31}$$

where the matrix $\mathbf{K}$ with elements $k_{i,n} = \tau_{n,i} A_n^{\tilde{\sigma}\sigma} U_n^{\tilde{\sigma}1-\sigma}$ is given by:

[43] For a review of random matrices, see Anderson et al. (2010) and for results on eigenvectors see Ben Arous and Guionnet (2010) and O'Rourke et al. (2016).

$$\mathbf{K} = \begin{bmatrix} k_{1,1} & k_{1,2} & \dots & k_{1,N} \\ k_{2,1} & k_{2,2} & \dots & k_{2,N} \\ \dots & \dots & \dots & \dots \\ k_{N,1} & k_{N,2} & \dots & k_{N,N} \end{bmatrix}$$

The random vector $\mathbf{h}$ is not the eigenvector of the random matrix $\mathbf{K}$. The vector $\mathbf{s}_i$ results from the multiplication of a random vector and a random matrix, motivating the treatment of elements $s_{n,i}$ as random variables.

A.5 Proofs for random fields

Several of our results generalize directly to geographies in two dimensions, as they necessitate an α-mixing sequence (as in the one-dimensional case) or otherwise do not depend on dimensions of the geography. This is true for Proposition 1 and Proposition 2 (which necessitate an α-mixing sequence) and Proposition 3 and Theorem 1 (which rely only on the properties of lognormal distributions).

The complication in considering geographies in two dimensions results when we must treat α-mixing random fields rather than α-mixing sequences. The additional complexity results from the need to be careful about the concept of "distance" within the sets and sequences when the index no longer neatly summarizes this information. The definition in Supplemental Appendix A.3 for α-mixing fields, for instance, defines the partition of the field into subsets by the Euclidean distance between the nearest elements of each subset.

To extend the proofs of Proposition 4 and Theorem 2 we show that the key properties of α-mixing sequences from Bradley (2005) Theorem 5.2 (which provides the proof for the main text case of sequences) can be extended to the case of α-mixing fields.

Lemma A.1: *Suppose that for each* $n = 1, 2, 3, ..., X^{(n)} := \left(X_k^{(n)}, k \in \mathbb{Z}^2\right)$ *is a (not necessarily stationary) field of random variables. Suppose these fields* $X^{(n)}$, $n = 1, 2, 3, ...$ *are independent of each other. Suppose that for each* $k \in \mathbb{Z}^2, h_k : \mathbb{R} \times \mathbb{R} \times \mathbb{R} \times \ldots \to \mathbb{R}$ *is a Borel function. Define the field* $X := (X_k, k \in \mathbb{Z}^2)$ *of random variables by* $X_k := h_k\left(X_k^{(1)}, X_k^{(2)}, X_k^{(3)}, \ldots\right), k \in \mathbb{Z}^2$. *Then for each* $m \geq 1$, $\alpha(X, m) \leq \sum_{n=1}^{\infty} \alpha\left(X^{(n)}, m\right)$

Proof: First, we want to show that α-mixing is preserved over measurable transformations of α-mixing random fields, and then we want to show that combinations of α-mixing random fields are also mixing. For brevity, we write $\alpha(k)$ in place of $\alpha(k; \infty, \infty)$ as appears in the definition of α-mixing fields in Supplemental Appendix A.3.

1. Define the field $\{\bar{D}_i\}$ such that for all $i \in \mathbb{Z}^2$, $\bar{D}_i = j\left(D_i^{(1)}, D_i^{(2)}, D_i^{(3)}, ...\right)$,

where $j(\cdot)$ is a measurable mapping that takes the field $\{D_i\}$, which is an n-tuple of random variables for each $i \in \bar{Z}$, as input. The field $\{D_i\}$ is α-mixing with respect to distance k. We want to show that the field $\{\bar{D}_i\}$ will be mixing as well. First note that

$$\mathbb{P}\left(\bar{D}_{s\in S} \in A, \bar{D}_{t\in T} \in B\right) = \mathbb{P}\Big((D^{(1)}_{s\in S}, D^{(2)}_{s\in S}, D^{(3)}_{s\in S}, ...) \in j^{-1}(A), \\ (D^{(1)}_{t\in T}, D^{(2)}_{t\in T}, D^{(3)}_{t\in T}, ...) \in j^{-1}(B)\Big)$$

And so,

$$\begin{aligned}
\alpha_{\bar{D}}(k) &= \sup_{A,B} \big|\mathbb{P}\left(\bar{D}_{s\in S*} \in A, \bar{D}_{t\in T*} \in B\right) \\
&\quad - \mathbb{P}\left(\bar{D}_{s\in S*} \in A\right)\mathbb{P}\left(\bar{D}_{t\in T*} \in B\right) \\
&= \sup_{A,B} |\mathbb{P}\left((D^{(1)}_{s\in S*}, ...) \in j^{-1}(A), (D^{(1)}_{t\in T*}, ...) \in j^{-1}(B)\right) \\
&\quad - \mathbb{P}\left((D^{(1)}_{s\in S*}, ...) \in j^{-1}(A)\right)\mathbb{P}\left((D^{(1)}_{t\in T*}, ...) \in j^{-1}(B)\right)| \\
&\leq \alpha_D(k),
\end{aligned}$$

as $\alpha_D(k)$ is defined as the supremum over sets S, T, not the fixed $S*, T*$ that correspond to $\{\bar{D}_i\}$. As $\alpha_D(k) \to 0$ as $k \to \infty$, then $\alpha_{\bar{D}}(k) \to 0$ as well and so $\{\bar{D}_i\}$ is α-mixing.

2. We now show that given two independent stationary random fields $\{Y_i\}, \{Z_i\}$ where $i \in \mathbb{Z}^2$ which are α-mixing with respect to distance k, the bivariate field $\{X_i\}$ where $X_i = (Y_i, Z_i)$ is also mixing.

   Define I:

$$\begin{aligned}
I &= |\mathbb{P}(X_{s\in S} \in A, X_{t\in T} \in B) - \mathbb{P}(X_{s\in S} \in A)\mathbb{P}(X_{t\in T} \in B)| \\
&= |\mathbb{P}((Y_{s\in S}, Z_{s\in S}) \in A, (Y_{t\in T}, Z_{t\in T}) \in B) \\
&\quad - \mathbb{P}((Y_{s\in S}, Z_{s\in S}) \in A)\mathbb{P}((Y_{t\in T}, Z_{t\in T}) \in B)|
\end{aligned}$$

Define

$$
\begin{aligned}
f(Z_{s\in S}, Z_{s\in T}) &= \mathbb{P}((Y_{s\in S}, Z_{s\in S}) \in A, (Y_{t\in T}, Z_{t\in T}) \in B) \\
g(Z_{S\in S}) &= \mathbb{P}((Y_{s\in S}, Z_{s\in S}) \in A) \\
h(Z_{t\in T}) &= \mathbb{P}((Y_{t\in T}, Z_{t\in T}) \in B)
\end{aligned}
$$

Substituting in and taking expectations,

$$
I = |\mathbb{E}[f(Z_{s\in S}, Z_{s\in T})] - \mathbb{E}[g(Z_{s\in S})h(Z_{t\in T})]|
$$

Add and subtract $\mathbb{E}[g(Z_{s\in S})]\mathbb{E}[h(Z_{t\in T})]$:

$$
\begin{aligned}
&= |\mathbb{E}[f(Z_{s\in S}, Z_{s\in T})] - \mathbb{E}[g(Z_{s\in S})]\mathbb{E}[h(Z_{t\in T})] \\
&\quad + \mathbb{E}[g(Z_{s\in S})]\mathbb{E}[h(Z_{t\in T})] - \mathbb{E}[g(Z_{s\in S})h(Z_{t\in T})]|
\end{aligned}
$$

Re-arrange and, using the $|\cdot|$,

$$
\begin{aligned}
&= |\mathbb{E}[f(Z_{s\in S}, Z_{s\in T})] - \mathbb{E}[g(Z_{s\in S})]\mathbb{E}[h(Z_{t\in T})] \\
&\quad - (\mathbb{E}[g(Z_{s\in S})h(Z_{t\in T})] - \mathbb{E}[g(Z_{s\in S})]\mathbb{E}[h(Z_{t\in T})])| \\
&\leq \underbrace{|\mathbb{E}[f(Z_{s\in S}, Z_{s\in T})] - \mathbb{E}[g(Z_{s\in S})]\mathbb{E}[h(Z_{t\in T})]|}_{II} \\
&\quad + \underbrace{|\mathbb{E}[g(Z_{s\in S})h(Z_{t\in T})] - \mathbb{E}[g(Z_{s\in S})]\mathbb{E}[h(Z_{t\in T})]|}_{III}
\end{aligned}
$$

Begin with II, where we use independence of Y, Z and mixing of Y to show

$$\begin{aligned}
II &= |\mathbb{E}[f(Z_{s\in S}, Z_{s\in T})] - \mathbb{E}[g(Z_{s\in S})\mathbb{E}h(Z_{t\in T})]| \\
&= |\mathbb{E}[\mathbb{P}((Y_{s\in S}, Z_{s\in S}) \in A, (Y_{t\in T}, Z_{t\in T}) \in B)] \\
&\quad - \mathbb{E}[\mathbb{P}((Y_{s\in S}, Z_{s\in S}) \in A)]\mathbb{E}[\mathbb{P}((Y_{t\in T}, Z_{t\in T}) \in B)]| \\
&= |\mathbb{E}[\mathbb{P}((Y_{s\in S}, Z_{s\in S}) \in A, (Y_{t\in T}, Z_{t\in T}) \in B | Z_{s\in S} = z_{s\in S}, Z_{t\in T} = z_{t\in T})] \\
&\quad - \mathbb{E}[\mathbb{P}((Y_{s\in S}, Z_{s\in S}) \in A | Z_{s\in S} = z_{s\in S})]\mathbb{E}[\mathbb{P}((Y_{t\in T}, Z_{t\in T}) \in B | Z_{t\in T} = z_{t\in T})]| \\
&= |\mathbb{P}(Y_{s\in S} \in A, Y_{t\in T} \in B) - \mathbb{P}(Y_{s\in S} \in A)\mathbb{P}(Y_{t\in T} \in B)|
\end{aligned}$$

Taking the supremum over A, B, we have

$$II \leq \alpha_Y(S, T)$$

Now consider III:

$$\begin{aligned}
III &= |\mathbb{E}[g(Z_{s\in S})h(Z_{t\in T})] - \mathbb{E}[g(Z_{s\in S})]\mathbb{E}[h(Z_{t\in T})]| \\
&= |Cov(g(Z_{s\in S}), h(Z_{t\in T}))|
\end{aligned}$$

Note that $\|g(Z_{s\in S})\|_\infty, \|h(Z_{t\in T})\|_\infty \leq 1$. By Lemma 3.1 of Doukhan (1994) and the α-mixing of $\{Z_t\}$ we have

$$III \leq 4\alpha_Z(S, T)$$

And so, putting together the above and, taking the supremum over A, B:

$$\alpha_X(S, T) \leq \alpha_Y(S, T) + 4\alpha_Z(S, T)$$

Taking the supremum again over all S, T such that $dist(S, T) \geq k$, we find

$$\alpha_X(k) \leq \alpha_Y(k) + 4\alpha_Z(k)$$

And, as we know $\alpha_Y(k), \alpha_Z(k) \to 0$ as $k \to \infty$, we have $\alpha_X(k) \to 0$ as $k \to \infty$ and so the field $\{X_i\}$ is mixing with respect to distance k.

Combining the results of Parts 1 and 2 establish the result. ■

With Lemma A.1, we can restate Proposition 4 and Theorem 2 for the case of random fields in two dimensions where $\{A_i\}$, $\{U_i\}$, Ω_i, and S_i are such that $i \in \mathbb{Z}^2$.

Proposition 4 (fields): *If $\{A_i\}$ and $\{U_i\}$, are independent α-mixing fields, then Ω_i is an α-mixing fields.*

Theorem 2 (fields): *If $\{\Omega_i\}\}$ and $\{S_i\}$ are independent α-mixing fields, then the population field $\{L_i\}$ is α-mixing.*

The proofs of both extensions follow directly from Lemma A.1.

B Pareto vs. Lognormal Simulations

We provide additional evidence for the lognormality of the true population by focusing on the behavior of the distribution in the tail. As discussed in Eeckhout (2004), one characteristic of the lognormal as compared to the Pareto is the sensitivity of the estimated coefficient to the truncation point. This can be see in Figure A.II, where selecting alternative truncation points changes the estimated power law coefficient. The left column consists of three plots where we estimate the power law coefficient on three different subsets of the U.S. city distribution. Panel A presents the same plot as main text Figure I. When including more cities (Panel C) the coefficient rises, and when including few cities (Panel E) the coefficient falls. This is in line with the expected behavior of the scale-varying "shape parameter"-like term of the lognormal distribution in Equation 3. The R^2 of all of these regressions remains similarly high. The changes in the estimated coefficient are in line with expectations if the true underlying distribution were lognormal and demonstrate that, while the -1 exponent can be found for a particular truncation point (as in Figure I), it does not appear to be a meaningful feature of the distribution.

In the right column of Figure A.II, we consider deviations in the far tail by excluding the top quarter of cities within each subset of the city distribution. In all cases, nearly all top quarter cities fall below the trendline predicted based on the rest of the distribution.[44] The magnitude of the systematic divergence is very large, which is obscured on the log scale. As noted in the main text, the total deviation below the trendline in Panel A is 76 million people missing from the top 250 U.S. MSAs, roughly a quarter of the U.S. population. The deviations are larger when estimated on the subset of cities below the top quarter as in Panels B, D, and F. If the Pareto were the true distribution, panel B indicates a cumulative absence (in expectation) of 412 million people while panel D indicates a cumulative 494 million people missing from the sets of cities considered, both substantially more than the entire U.S. population,

[44] Of top-quarter MSAs, 62 of 62 MSAs in Panel B, 93 of 96 MSAs in panel D, and 27 of 27 MSAs in panel F are below the respective trendlines in Figure A.II

while panel F indicates an absence of 169 million people, roughly half the U.S. population.[45]

This scale variance offers evidence for the lognormal interpretation of the population distribution. When the true population is lognormal, large economies or regions (those containing many cities) should systematically contain smaller large cities than predicted by the estimated power law. We first demonstrate this property of the two distributions via simulation in Figure A.III. We calibrate a lognormal distribution to match a Pareto distribution with shape parameter $\alpha_P = 1$ in the tail.[46] The plots show the average value over 10000 draws from each distribution at each rank of the city size distribution, with the bands reflecting the 95 percent confidence interval. We calculate the slope at several scales excluding the top 25% of cities, to demonstrate the tail divergence of the lognormal resulting from its scale-variance, in contrast to the scale-invariant Pareto. When the tail is constructed to contain 100 cities, the difference between the two plots is minimal. However, when the tail is constructed to have 800 cities, cities in the far tail of the lognormal fall well below the estimated trendline.

[45]Repeating this exercise with other large countries (India, China, and Brazil) using standardized city definitions from Dingel et al. (2021) indicates similarly large divergences in the tail, all in the expected direction (cumulative absences of 135 million, 53 million, and 8 million respectively).

[46]The lognormal parameter $\sigma_{LN} = 2.6$ used for these simulations is similar to that resulting from simulation of the model (in Section 4) for standard parameter values in the literature. This value is larger than that identified by Eeckhout (2004) (who finds $\sigma_{LN} = 1.75$). The difference could partially be attributed to differing truncation points, along with the empirical difficulty of evaluating the population of small locations and the lower bound on real-world populations of 1.

C Data and Empirical Results

C.1 Data

In this section, we list the variables we used in Section 3 for our correlation matrices and tables. The data come from the publicly-available data of Henderson et al. (2018).

1. *Ruggedness:* index measure of local variation in elevation. Originally computed by Nunn and Puga (2012) with corrections made in Henderson et al. (2018).
2. *Elevation:* above sea level, meters
3. *Temperature:* average from 1960-1990 of monthly temperatures, Celsius
4. *Precipitation:* average from 1960-1990 of monthly total precipitation, mm/month
5. *Land Suitability:* propensity of an area of land to be under cultivation based on separate measures of climate and soil quality
6. *Distance to Coast:* distance to the nearest coast, km
7. *Distance to Harbor:* distance to nearest natural harbor on the coast, km (great circle)
8. *Distance to River:* distance to nearest navigable river, km
9. *Malaria:* index of the stability of malaria transmission
10. *Land Area:* grid cell area covered by land, km^2
11. *Growing Days:* Length of agricultural growing period, days/year

Figure A.II:
Truncation Points and Power Law Coefficients

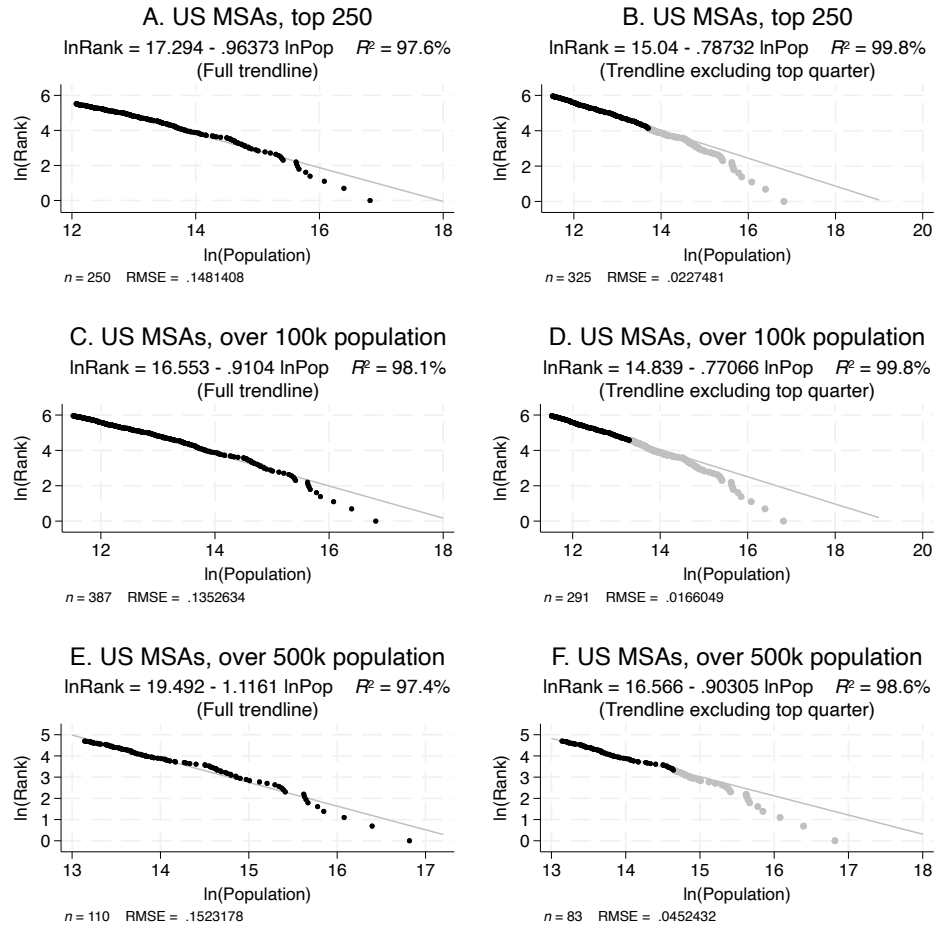

Notes: The top panels (A and B) show the 388 U.S. MSAs with a population over 100k in 2020. The bottom panels (C and D) show the 110 MSAs with a population over 500k in 2020. Panels A and C display the trendline for the full distribution and Panels B and D display the trendline excluding the top 25% of MSAs (in orange) in each panel. Altering the truncation point substantially influences the estimated coefficient, as can be seen by contrasting Panels A and C with Figure I Further, nearly all top quartile MSAs falling below the trendline (94 of 97 MSAs in panel B and 27 of 27 MSAs in panel D are below the respective trendlines). Both are consistent with the U.S. population distribution being lognormal.

Data Source: U.S. Census

Figure A.III:
Comparison of Lognormal and Pareto Distributions of Cities

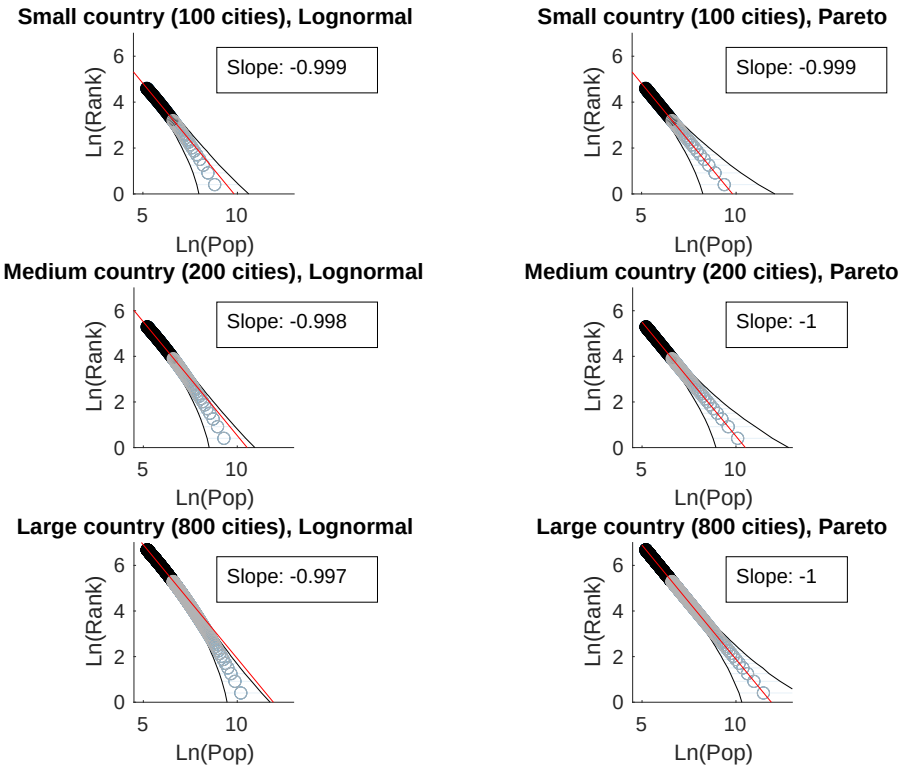

Notes: Comparison of Lognormal (left) and Pareto (right) for simulated small, medium, and large "countries." The LN is truncated for cities 2 standard deviations above μ_{LN}, and the Pareto has a minimum value equivalent to this truncation point with shape parameter $\alpha_P = 1$. The slope in each plot is calculated excluding the top 25% of cities in each country, and the bands contain 95% of the observed values at each rank over 1000 simulations. At small scales, the lognormal distribution at Pareto distribution are largely indistinguishable. However, scale variance of the LN leads to substantial divergence in the tail. At larger scales (large countries with more large cities), if the distribution is draw from a LN distribution the large cities tend to fall below the trendline (with trend above the 95% band) while the the Pareto distribution does not diverge.

C.2 Summary Statistics

We provide summary statistics of our attributes in Table A.I.

Table A.I: Summary Statistics for Attributes

Variable	N	Min	Max	Median	Q1	Q3	IQR	Mean	SD
Ruggedness	13,426	−2.65	1.79	0.06	−0.69	0.71	1.40	0.00	1.00
Elevation	13,426	−3.02	1.99	−0.06	−0.71	0.92	1.63	0.00	1.00
Land Suitability	13,426	−2.77	1.13	0.14	−0.55	0.91	1.46	0.00	1.00
Dist to River	13,426	−1.38	10.75	−0.25	−0.69	0.39	1.08	0.00	1.00
Dist to Coast	13,426	−0.90	4.98	−0.32	−0.60	0.23	0.84	0.00	1.00
Temperature	13,426	−3.15	2.29	−0.08	−0.76	0.83	1.60	0.00	1.00
Precipitation	13,426	−2.53	3.46	−0.12	−0.89	0.78	1.67	0.00	1.00
Dist to Harbor	13,426	−1.16	5.38	−0.32	−0.74	0.46	1.21	0.00	1.00
Growing Days	13,426	−3.12	1.54	−0.04	−0.84	0.88	1.72	0.00	1.00
Malaria Ecology	13,426	−5.60	0.56	0.51	−0.35	0.56	0.91	0.00	1.00
Land Area	13,426	−17.66	0.59	0.16	−0.03	0.32	0.34	0.00	1.00

Notes: Summary statistics for ordered geographic attributes for data points in the contiguous United States.
Data Source: Authors' calculations using data from Henderson et al. (2018)

C.3 Correlation Calculations

Cross-Correlations For every attribute type g, we calculate $corr(\boldsymbol{a_i}, \boldsymbol{a_j}),\ \forall i, j \in \mathcal{G},\ j \neq g$, where $\boldsymbol{a_g}$ is a vector for each attribute type comprised of attribute values a_{ig} for every location i. This exercise tells us how correlated each attribute is with each other attribute within locations, giving an indication of how dependent realizations of geographic attributes may be on one another.[47]

Spatial Correlation To calculate spatial correlations within attributes, we construct rings at varying distances d (in miles) from every grid cell i in the contiguous U.S.; we refer to a location i around which rings are being drawn as a *centroid*. These rings define a collection of grid points in the U.S., Canada, and Mexico at a given buffered distance $(d-10, d+10)$ for each centroid.[48] We then select a random point, called $i^*(d, g)$, from within each ring of distance d from every centroid i, to construct our sets of points to calculate the correlations; we re-draw a random point for each attribute type g for every centroid. Mathematically, our calculation for the correlation within an attribute type g between our set of centroids and our set of points at distance d takes the form $corr(\boldsymbol{a_g}, \boldsymbol{a_{dg}}),\ \forall g \in \mathcal{G},\ \forall d$, where $\boldsymbol{a_g}$ is a vector of attribute values a_{ig} for attribute type g for all centroid locations i in our sample, and $\boldsymbol{a_{dg}}$ is a vector of all attribute values $a_{i^*(d,g)g}$, the randomly-selected points for each centroid i at distance d for each attribute type g.

[47] We do not know the full suite of attributes that characterize a location's productivity, and in our limited panel we have some attributes which are mechanically correlated within a location (such as average temperature and growing days).

[48] The spatial correlation in attributes between points at distance $d = 100$ miles should be interpreted as "the correlation between a point and a randomly-selected point 90–110 miles away". The buffer is to ensure there are eligible points at roughly the desired distance.

C.4 Empirics of Attribute Correlations

We empirically investigate the correlation of pairs of attributes within locations and the correlation of attributes across space. We provide support for our assumption of α-mixing for attributes within a place, used to apply the central limit theorem above to characterize the fundamentals, and the assumption of α-mixing of attributes across space, which will be used in Section 3 to characterize the population distribution.

We use gridded geographic data from Henderson et al. (2018), which includes a wide variety of first-nature geographic attributes of which we use the eleven continuous variables.[49] The dataset is at the quarter-degree latitude and longitude cell level.[50] We focus on the roughly 47,000 cells grid cells in the U.S., Mexico, and Canada, with the nearly 13,000 of those grid cells contained in the contiguous U.S. serving as our main sample.[51]

First, we calculate the correlation between attributes within a given location and show that weak dependence of attributes is a reasonable assumption, as there exist pairs of attributes which do not appear correlated within places. We calculate cross-correlations between our attributes for all grid cells in the contiguous U.S., as shown in Figure A.IVa.[52] Our results show that the assumption of weak dependence of attributes appears reasonable given the pattern of correlations of attributes within locations. While there appears to be some correlation between some pairs of attributes within locations, the median correlation among the least-correlated attribute pairs is very near 0.

[49]The variables are ruggedness, elevation, land suitability for cultivation, distance to a river, distance to an ocean coast, average monthly temperature, average monthly precipitation, distance to a natural harbor, growing days per year, an index of malaria, and total land area of the grid cell. Variables in Henderson et al. (2018) which were either categorical or discrete transformations of the continuous data were excluded from our analysis.

[50]At the equator, a grid cell is ≈28-by-28 km; at 48 degrees latitude, ≈18-by-18 km.

[51]The reduction in the number of attributes and geographic scope does not drastically decrease the explanatory power of the attributes on economic activity relative to Henderson et al. (2018); see Supplemental Appendix Table A.III for a regression showing that our eleven attributes explain 43% of the variance in economic activity in the contiguous U.S., in line with the 47% Henderson et al. (2018) found globally with their full set of attributes.

[52]A description of how we calculated cross-correlation is provided in Supplemental Appendix C.3

Figure A.IV:
Correlations Within and Across Locations

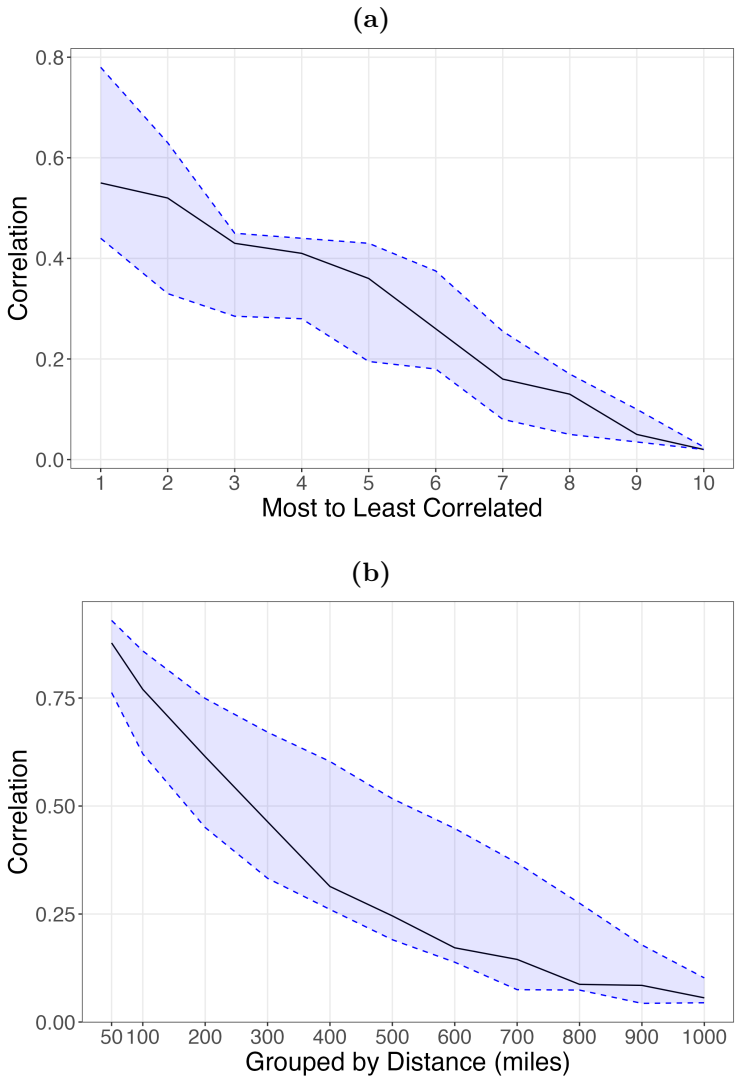

Notes: (a) Cross-correlation and (b) spatial correlation structure of U.S. geographic attributes. The solid black line represents the median correlation; the blue dashed lines represent the 25th and 75th percentile bands.
Data Source: Authors' calculations using data from Henderson et al. (2018)

Next, we demonstrate that while there is correlation within each attribute across space, this correlation declines to zero as distance increases. We cal-

culate spatial correlation at various distances for grid points within the contiguous U.S., as seen in Figure A.IVb.[53] The spatial correlation of attributes is high over short distances but as distance increases spatial correlation falls to near zero. These results suggest spatial correlation of geographic attributes does decline with distance, supporting the assumption that the fundamentals will exhibit a similar pattern of declining correlation across space.

[53] A description of how we calculated spatial correlation is provided in Supplemental Appendix C.3.

C.5 Calculating the Fundamental

For every attribute in our data set which has a minimum value less than or equal to 0, we re-define the attribute using an affine transformation to put the minimum ≈0.1. We then construct the "worst-to-best" ordering of our attribute values according to the sign on each attribute from a regression on attribute influence on economic activity as found in Henderson et al. (2018), Table 1. Attributes whose sign was positive we perform no additional transformations to. Attributes whose sign was negative we invert. We use the signs present in that table, as opposed to signs from a smaller regression of our subset of attributes on U.S. economic activity, because we believe the signs in their regression could plausibly be more robust world-wide.

After choosing our attribute value ordering, we then standardize the natural log of our attributes:

$$\frac{\ln(a_{ig}) - \text{mean}\left(\ln(a_g)\right)}{\text{sd}(\ln(a_g))}$$

where $\text{mean}\left(\ln(a_g)\right)$ is the mean of that attribute across all locations and $\text{sd}\ln(a_g)$ is the standard deviation. This produces logged attributes which are mean 0 and standard deviation 1.

We then aggregate our attributes into a fundamental given by Equation 22:

$$\ln(A_i) = \sum_{g \in \mathcal{G}} \xi_g \ln(a_{ig})$$

setting $\xi_g = 1,\ \forall g$.

C.6 Results: Fundamental and Correlations

Figure A.V:
Lognormal Distribution of Locational Fundamentals for Contiguous United States

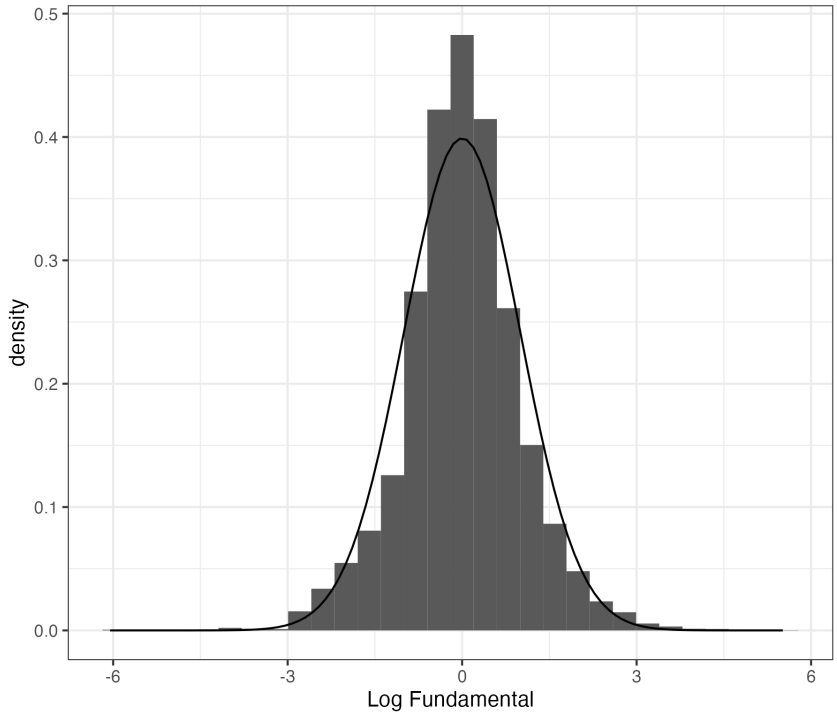

Notes: Lognormal distribution of locational fundamentals. All eleven attributes were ordered worst to best in terms of contribution to economic activity, logged, then standardized. The fundamental is calculated as the standardized sum of the standardized, ordered log attributes. The mean and variance are standardized to zero and one and a standard normal curve is overlaid.
Data Source: Authors' calculations using data from Henderson et al. (2018)

We plot in Figure A.V the empirical PDF of the resulting distribution of productivity fundamentals, calculated according to Equation 22 with $\xi_g = 1$, $\forall g$. The log of the empirical "fundamental" here is closely fit by a normal distribution, supporting the claim that aggregating weakly dependent and spatially correlated attributes can result in lognormal fundamentals, both in theory and in the data.

Table A.II: Spatial Correlation of Calculated Fundamental for the Contiguous United States

Distance (miles)	Correlation
50	0.66
100	0.50
200	0.30
300	0.17
400	0.05
500	0.02
600	-0.01
700	-0.06
800	-0.07
900	-0.04
1000	-0.03

Notes: The table indicates declining correlation towards 0 over distance of our logged fundamental, in line with theoretical predictions. Given randomness in the correlation calculation process, spurious and small deviations from 0 at large distances are possible.
Data Source: Authors' calculations based on data from Henderson et al. (2018).

Additionally, we calculate the spatial correlation of the logged fundamental over distance for the contiguous U.S. The table of correlation values, provided in Table A.II, shows declining correlation over distance, consistent with our theoretical predictions and in line with the spatial correlation declines which appear for geographic attributes (provided in the main text).

C.7 Regression of Economic Activity on Attributes

We provide regression results in Table A.III for economic activity on our eleven attributes for a sample including all points in the contiguous United States, interpreting the R^2 as suggestive evidence of the reasonably large explanatory power first nature geographic attributes on economic activity.

Table A.III: Regression of Economic Activity on Attributes

	Dependent variable:
	(Log of) Radiance
(Inv) Ruggedness	0.104
	(0.020)
Elevation	−1.279
	(0.057)
Land Suitability	0.298
	(0.039)
(Inv) Dist to River	−0.079
	(0.024)
(Inv) Dist to Coast	−0.135
	(0.034)
Temperature	−0.607
	(0.195)
(Inv) Precipitation	0.357
	(0.082)
(Inv) Dist to Harbor	0.006
	(0.049)
Growing Days	1.722
	(0.090)
(Inv) Malaria	−0.060
	(0.046)
Land Area	0.401
	(0.068)
Constant	−0.340
	(1.102)
Observations	13,426
R^2	0.431
Adjusted R^2	0.430
Residual Std. Error	2.294 (df = 13414)
F Statistic	922.395 (df = 11; 13414)

Notes: Grid-cell radiant lights on attributes, contiguous United States. (Inv) indicates the attribute data was inverted. The R^2 from this regression is comparable to the main regression from Henderson et al. (2018).

Data Source: Authors' calculations based on data from Henderson et al. (2018)

C.8 Recovered fundamentals from Allen and Arkolakis (2014)

We plot the exogenous productivity and amenity values recovered in Allen and Arkolakis (2014). These are at the county-level. County populations are roughly lognormally distributed, as seen in Figure A.VI. The resulting fundamentals recovered by Allen and Arkolakis (2014), as seen in Figure A.VII, also appear roughly lognormally distributed. The correlation between A and u is roughly 0.12, which one can use to parameterize our simulations.

Figure A.VI:
Distribution of Logged County Population in the United States

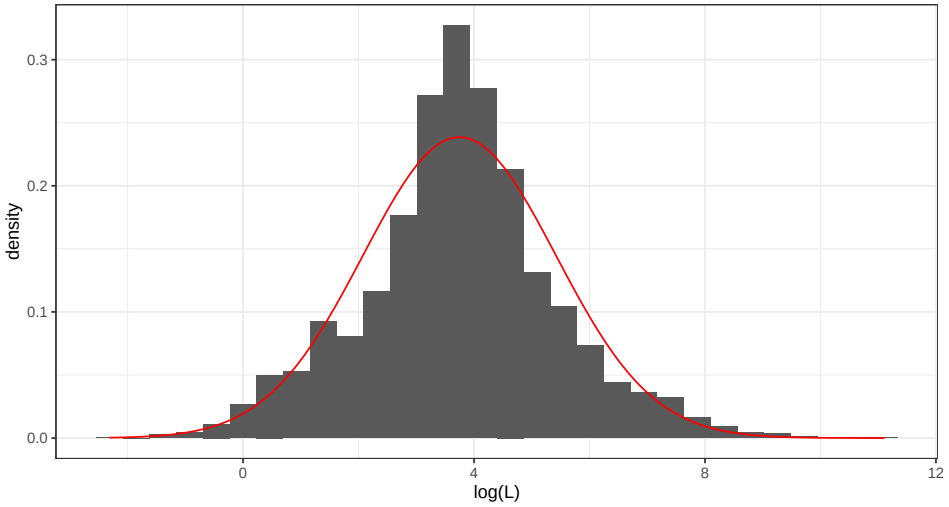

Notes: Distribution of logged county populations (L) in the United States, with superimposed normal curve. Number of counties N=3,109.
Data Source: online replication package from Allen and Arkolakis (2014).

Figure A.VII:
Distribution of Fundamentals in United States

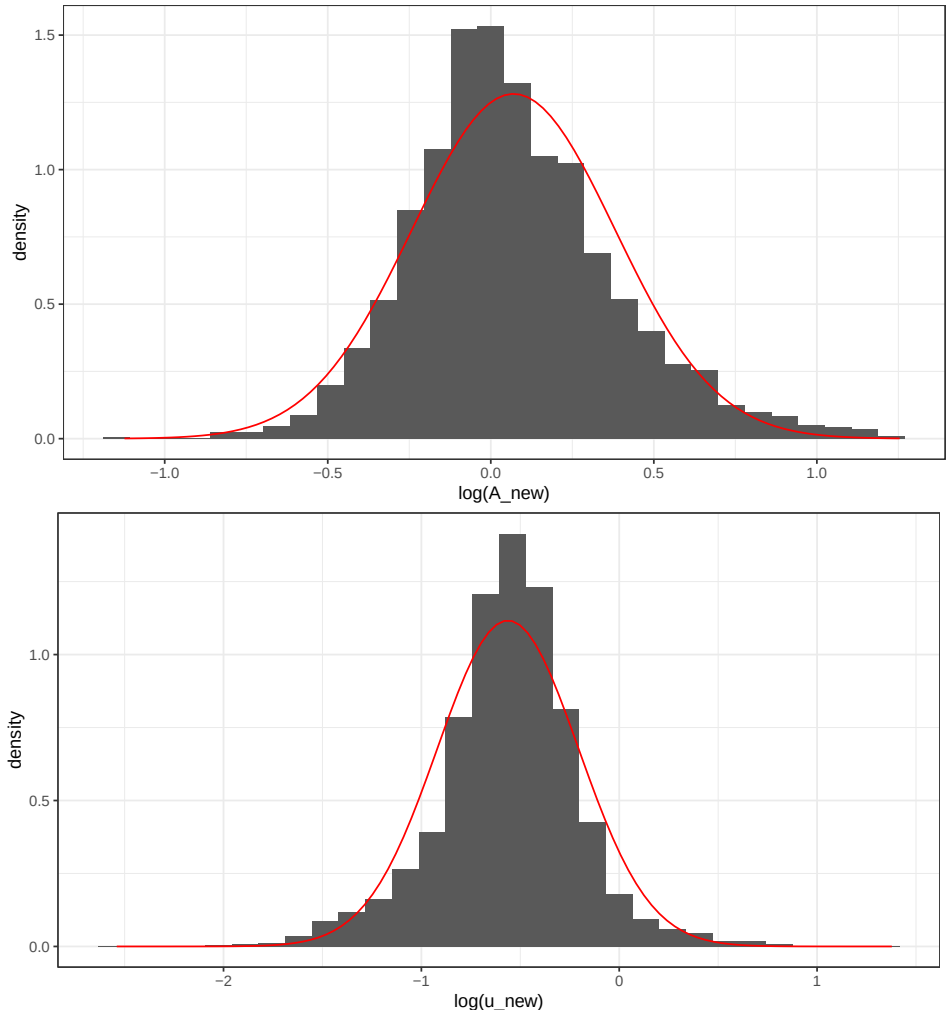

Notes: Top panel shows distribution of logged exogenous productivities (A_{new}) at the county-level in the United States, with super-imposed normal curve. Bottom panel shows distribution of logged exogenous amenities (u_{new}) at the county-level in the United States, with super-imposed normal curve. Number of counties N=3,109.
Data Source: online replication package from Allen and Arkolakis (2014).

Figure A.VIII:
Example of "Dartboard" Geography

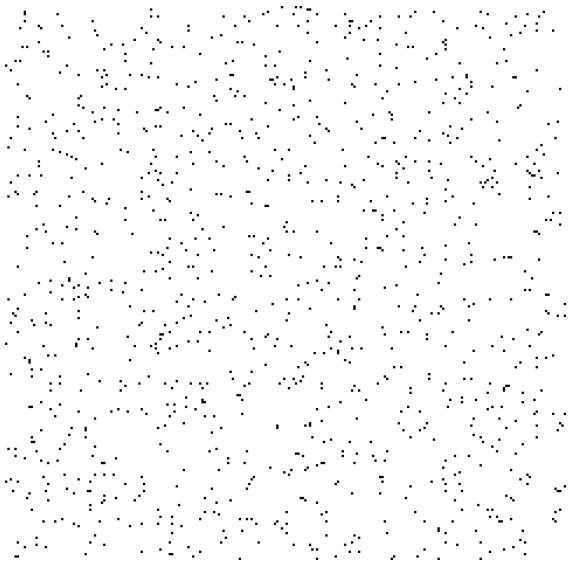

Notes: The figure shows the middle settlements of our full geography to provide an example of how we induce variation in trade costs.

D Additional Simulated Results

D.1 Example of "dartboard" geography

In our simulated results we first randomly generate a dartboard geography to ensure dispersion in trade costs. We take draws from uniform distributions with parameters $[0, a]$ where a reflects the maximal horizontal and vertical dimension of our full square geography. We take draws until we have realized a set number of locations within the full geography. Figure A.VIII shows the locations in the center of our full geography to provide an example of the realized "dartboard." Using a dartboard geography is convenient because it allows us to ensure trade costs respect the triangle inequality, ensures random variation in trade costs, and obviates the need to calculate least-costs paths beyond taking the Euclidean distance between points.

D.2 The distribution of S_i

Our proof has two implications for the distribution of S_i, the "market access" term in the equilibrium population condition, in simulation that we verify here. First, by Lemma 1, Theorem 1 implies that S_i will appear distributed normally in both levels and logs. Second, Theorem 1 and Theorem 2 require that $S_i^{\frac{1}{\tilde{\sigma}\gamma_1}}$ is independent of Ω_i.

We demonstrate that the first property holds by plotting the histogram of values of S_i for a given geography in both logs and levels, along with the respective QQ plots comparing both to a normal distribution, in Figure A.IX. The distribution in Figure A.IX displays the expected patterns, with a good fit to the normal distribution in both levels and logs as implied by Theorem 1. The smaller than expected right tail may be attributable to too little dispersion in trade costs or the size of the grid we simulate.

To check independence, we verify that the average correlation between Ω_i and $S_i^{\frac{1}{\tilde{\sigma}\gamma_1}}$ over the 1000 replications is 0.017, indicating the two terms are virtually uncorrelated as implied by the proof. While not a sufficient condition for independence, no correlation is necessary condition.

We take these simulated results as evidence that the mechanism we emphasize in our proofs is the mechanism driving the result. Further, we note that the setting we used for our simulation has very little variation in trade costs compared to a more realistic geography. Greater variation should be expected to increase the fit of the simulated S_i to the expected distribution and reduce the correlation of Ω_i and $S_i^{\frac{1}{\tilde{\sigma}\gamma_1}}$, as shown in Supplemental Appendix D.4.

Figure A.IX:
Distribution of Sums

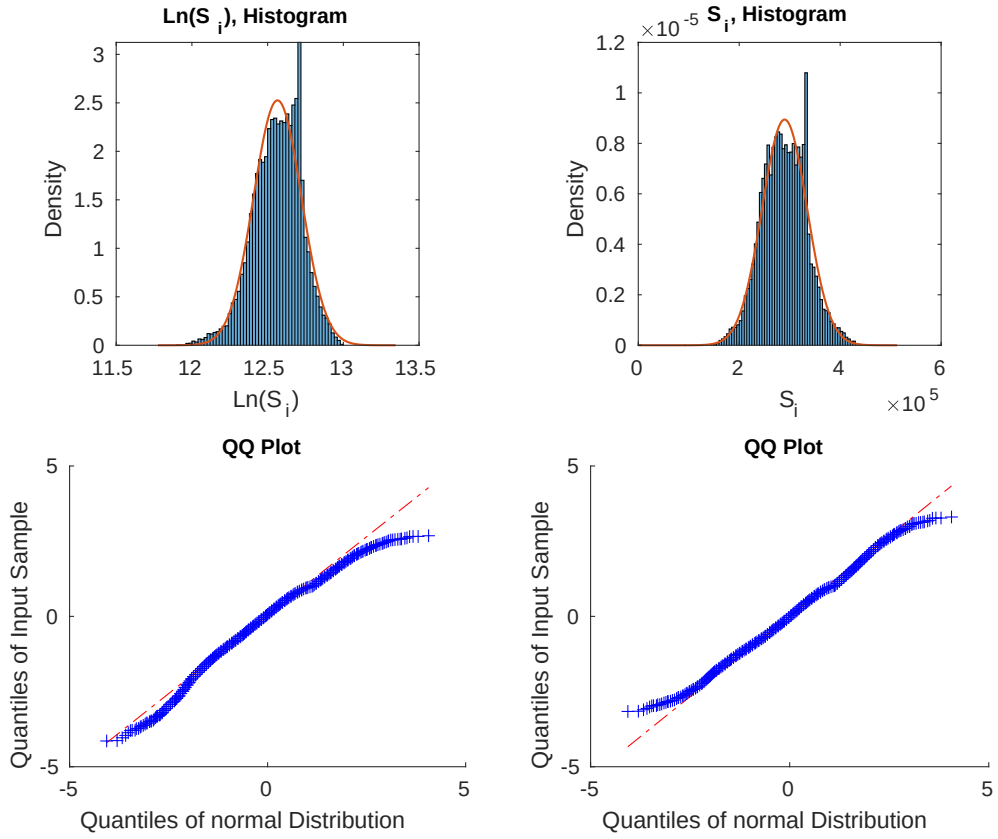

Notes: The figures above show a realization of the vector of S_i terms for some exogenous geography and associated population vector. The distribution of S_i appears normal in both levels and logs.

D.3 Additional simulations: Varying Parameter Values

In the simulations for varying parameter values, we take all combinations of $\alpha = [0.02, 0.04, 0.06, 0.08, 0.1]$, $\beta = [-0.25, -0.30, -0.35, -0.40, -0.45, -0.50]$, and
$\delta_{TC} = [0.0005, 0.001, 0.0015, 0.002, 0.0025]$. For each combination, we find the population distribution for 100 draws of the exogenous geography in a grid of the same dimensions as for our main results. We set the number of locations in the full geography to 10000.

We here report the full table of estimated parameter values for three values of δ_{TC}, at 0.0005, 0.0015, and 0.0025. When increasing α, the coefficient tends to increase (flatter slope). When increasing β, the coefficient tends to decrease (steeper slope). When increasing δ_{TC}, the coefficient tends to increase (flatter slope). As can be seen in Tables A.IV (showing average coefficients) and A.V (showing median coefficients) the change is nearly always in the anticipated direction.

To get the comparative statics reported in Table II, using the average estimated coefficient $\hat{\theta}_i$ from each of the 150 combinations of parameters we estimate the following regression:

$$\hat{\theta}_i = \psi_1 \alpha_i + \psi_2 \beta_i + \psi_3 \delta_{TC,i} + \epsilon_i \tag{32}$$

where the estimated coefficients $\hat{\psi}_1$, $\hat{\psi}_2$, and $\hat{\psi}_3$ are estimates of $\frac{\partial \theta_1}{\partial \alpha}$, $\frac{\partial \theta_1}{\partial \beta}$, and $\frac{\partial \theta_1}{\partial \theta}$, respectively. The signs of these coefficients are reflected in Table II, and the full regression output is included in Table A.VI.

Notably, the estimated coefficients are consistently in the neighborhood of -1 throughout the parameter space we simulate here. Given alternative truncations of the distribution (either expanding or reducing the number of locations included, as discussed in Gibrat (1931)) achieving a -1 slope is likely possible for most of these parameter combinations.

Table A.IV: Changes to Mean Power Law Coefficient through Model Parameters

Panel A: $\delta_{TC} = 0.0005$

	$\beta = 0.25$	$\beta = 0.30$	$\beta = 0.35$	$\beta = 0.40$	$\beta = 0.45$	$\beta = 0.50$
$\alpha = 0.02$	–0.750	–0.842	–0.928	–1.013	–1.109	–1.181
	(0.034)	(0.030)	(0.036)	(0.043)	(0.035)	(0.046)
$\alpha = 0.04$	–0.718	–0.813	–0.899	–0.980	–1.075	–1.152
	(0.027)	(0.032)	(0.037)	(0.036)	(0.044)	(0.040)
$\alpha = 0.06$	–0.696	–0.778	–0.875	–0.953	–1.050	–1.134
	(0.029)	(0.030)	(0.034)	(0.039)	(0.035)	(0.050)
$\alpha = 0.08$	–0.665	–0.757	–0.841	–0.928	–1.014	–1.101
	(0.026)	(0.028)	(0.035)	(0.042)	(0.038)	(0.042)
$\alpha = 0.10$	–0.640	–0.724	–0.819	–0.899	–0.990	–1.072
	(0.029)	(0.029)	(0.029)	(0.036)	(0.036)	(0.041)

Panel B: $\delta_{TC} = 0.0015$

	β = -0.25	β = -0.30	β = -0.35	β = -0.40	β = -0.45	β = -0.50
$\alpha = 0.02$	–0.736	–0.828	–0.917	–1.002	–1.091	–1.183
	(0.032)	(0.032)	(0.038)	(0.038)	(0.041)	(0.051)
$\alpha = 0.04$	–0.708	–0.794	–0.886	–0.969	–1.052	–1.142
	(0.032)	(0.032)	(0.037)	(0.042)	(0.042)	(0.046)
$\alpha = 0.06$	–0.683	–0.769	–0.852	–0.942	–1.025	–1.116
	(0.032)	(0.037)	(0.036)	(0.038)	(0.043)	(0.045)
$\alpha = 0.08$	–0.640	–0.738	–0.827	–0.918	–1.008	–1.094
	(0.030)	(0.031)	(0.032)	(0.041)	(0.043)	(0.043)
$\alpha = 0.10$	–0.614	–0.711	–0.799	–0.889	–0.977	–1.066
	(0.035)	(0.030)	(0.037)	(0.036)	(0.040)	(0.040)

Panel C: $\delta_{TC} = 0.0025$

	β = -0.25	β = -0.30	β = -0.35	β = -0.40	β = -0.45	β = -0.50
$\alpha = 0.02$	–0.714	–0.811	–0.901	–0.982	–1.080	–1.166
	(0.047)	(0.035)	(0.039)	(0.043)	(0.046)	(0.046)
$\alpha = 0.04$	–0.688	–0.772	–0.863	–0.959	–1.044	–1.127
	(0.033)	(0.035)	(0.038)	(0.038)	(0.045)	(0.049)
$\alpha = 0.06$	–0.657	–0.747	–0.830	–0.922	–1.021	–1.106
	(0.034)	(0.033)	(0.041)	(0.038)	(0.047)	(0.051)
$\alpha = 0.08$	–0.624	–0.717	–0.804	–0.886	–0.986	–1.075
	(0.032)	(0.035)	(0.035)	(0.034)	(0.041)	(0.050)
$\alpha = 0.10$	–0.593	–0.683	–0.776	–0.867	–0.954	–1.044
	(0.034)	(0.032)	(0.034)	(0.042)	(0.035)	(0.042)

Notes: Table containing the average coefficient over 100 simulations on the exogenous geography. The standard deviation of the estimated coefficient over the 100 simulations is in parenthesis.

Table A.V: Changes to Median Power Law Coefficient through Model Parameters

Panel A: $\delta_{TC} = 0.0005$

	β = -0.25	β = -0.30	β = -0.35	β = -0.40	β = -0.45	β = -0.50
$\alpha = 0.02$	–0.748	–0.850	–0.928	–1.023	–1.113	–1.191
$\alpha = 0.04$	–0.719	–0.813	–0.903	–0.986	–1.077	–1.156
$\alpha = 0.06$	–0.703	–0.789	–0.879	–0.955	–1.051	–1.139
$\alpha = 0.08$	–0.672	–0.763	–0.851	–0.930	–1.019	–1.109
$\alpha = 0.10$	–0.648	–0.725	–0.823	–0.904	–0.993	–1.078

Panel B: $\delta_{TC} = 0.0015$

	β = -0.25	β = -0.30	β = -0.35	β = -0.40	β = -0.45	β = -0.50
$\alpha = 0.02$	–0.742	–0.833	–0.918	–1.004	–1.093	–1.190
$\alpha = 0.04$	–0.714	–0.790	–0.898	–0.976	–1.057	–1.151
$\alpha = 0.06$	–0.689	–0.770	–0.859	–0.951	–1.027	–1.119
$\alpha = 0.08$	–0.658	–0.741	–0.829	–0.932	–1.015	–1.100
$\alpha = 0.10$	–0.618	–0.713	–0.801	–0.900	–0.987	–1.075

Panel C: $\delta_{TC} = 0.0025$

	β = -0.25	β = -0.30	β = -0.35	β = -0.40	β = -0.45	β = -0.50
$\alpha = 0.02$	–0.733	–0.817	–0.903	–0.992	–1.089	–1.170
$\alpha = 0.04$	–0.697	–0.765	–0.865	–0.965	–1.046	–1.141
$\alpha = 0.06$	–0.671	–0.756	–0.830	–0.925	–1.027	–1.117
$\alpha = 0.08$	–0.610	–0.728	–0.808	–0.895	–0.996	–1.089
$\alpha = 0.10$	–0.601	–0.692	–0.783	–0.881	–0.957	–1.061

Notes: Table containing the median coefficient over 100 simulations on the exogenous geography.

Table A.VI: Estimated Coefficients from Regression 32

	(1)
α	1.449***
	(0.0131)
β	1.769***
	(0.00433)
δ_{TC}	16.72***
	(0.523)
adj. R^2	0.999
N	150

Standard errors in parentheses
* $p < 0.10$, ** $p < 0.05$, *** $p < 0.01$

Table A.VII: Normality Tests, "Idiosyncratic" Distance Simulations

	Kolmogorov-Smirnov	Lilliefors	Jarque-Bera
Rejected at 1%	0.000	0.010	0.013
Rejected at 5%	0.000	0.042	0.075

Notes: Table shows the share of tests for a normal distribution rejected for the log equilibrium population of 1000 Monte-Carlo simulations.

D.4 Simulation with idiosyncratic shocks to effective distance

Variation in trade costs across locations are likely substantially greater than in the simple geography we simulate in our main specification. Consider the low trade costs for locations along natural bodies of water or along man-made transportation networks such as canals, train lines, or roadways. Trade costs can also vary for locations-specific idiosyncratic reasons such as policy (tariffs on broad categories of goods and other trade barriers) or bilateral factors that encourage or discourage trade (tariffs on particular countries or shared language).

In this appendix section we show that inducing additional variation in realized trade costs improves the simulated results relative to the more restrictive baseline we presented in the main paper. We here consider the potential for trade costs to vary for idiosyncratic location-specific and bilateral reasons.

We here simulate with $\tau_{i,n} = \exp(\delta_{TC}\beta_i\beta_{i,n}d_{i,n})$, where $\beta_i \in (0,1)$ and $\beta_{i,n} \in (0,1)$. We draw all β_i and $\beta_{i,n} = \beta_{n,i}$ from a uniform (0,1) distribution. The parameter values are the same as in our baseline results and we simulate for 10,000 locations as in the Monte Carlo results.

Notably, the lognormality of the resulting population distribution is rejected less frequently than in our baseline results. The distribution of S_i is also appreciably more lognormal when including additional variation in effective distance than in baseline.

Figure A.X:
Example of the Equilibrium Population Distribution, "Idiosyncratic" Distance

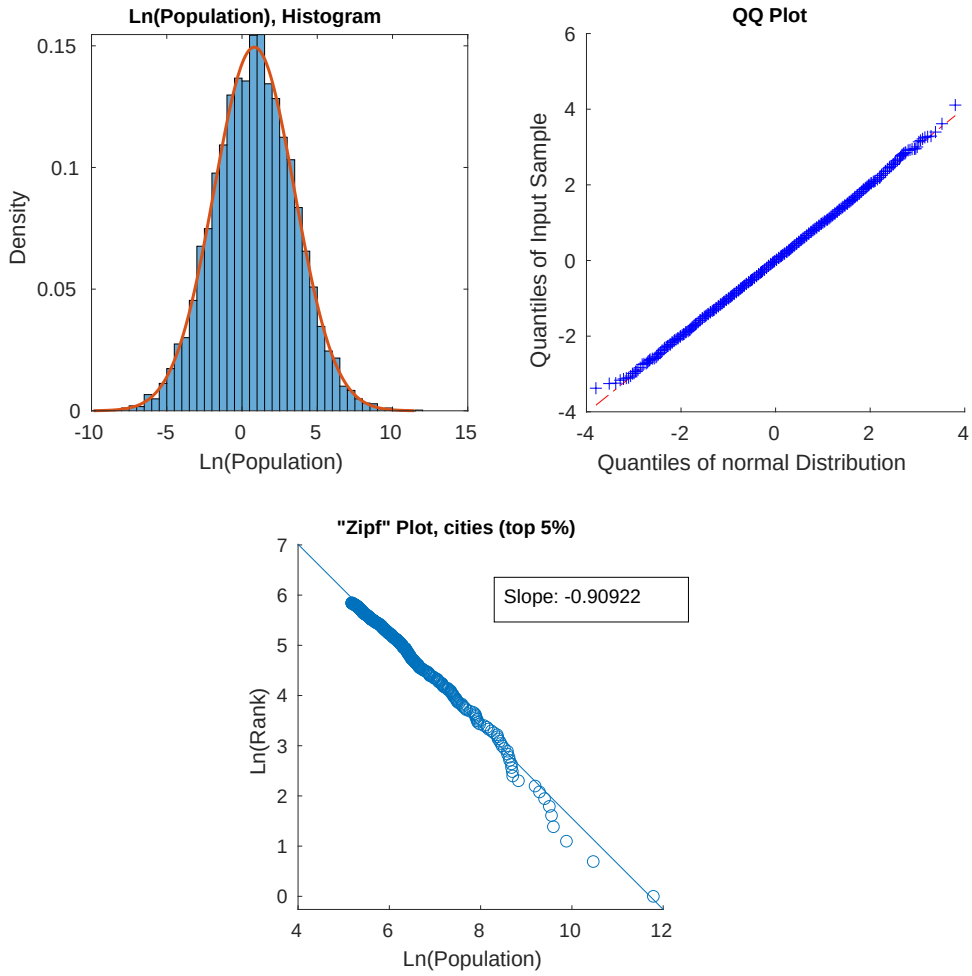

Notes: The top left panel shows the model's log population appears to follow a normal distribution. The top right panel contains a QQ plot of the model's log population distribution, indicating that it very closely matches a normal distribution. The log rank-size plot at the bottom shows a strong resemblance to the typical log rank-size plot for cities along with the characteristic divergence of the largest locations below the trendline.

Figure A.XI:
Distribution of S_i, Market Access Term, "Idiosyncratic" Distance Simulation

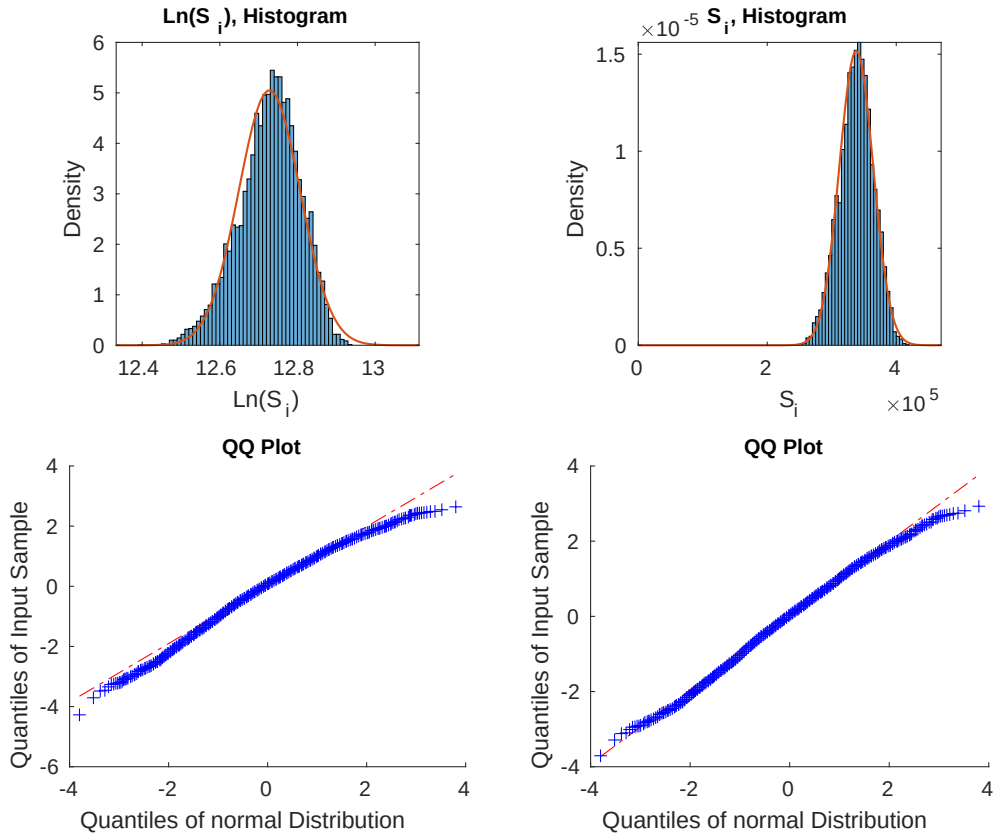

Notes: The figures above show a realization of the vector of S_i terms for some exogenous geography and associated population vector. The distribution of S_i appears normal in both levels and logs.

Figure A.XII:
Smoothed Output Over 1000 MC Simulations, "Idiosyncratic" Dist.

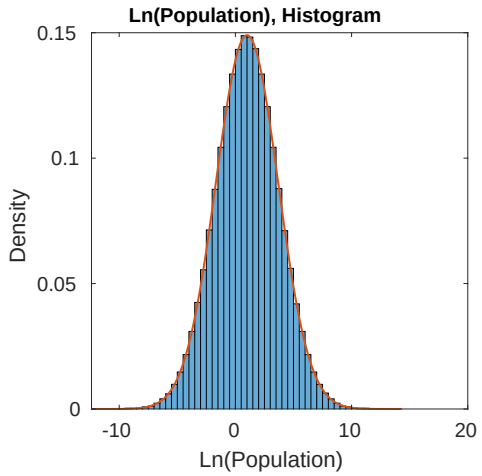

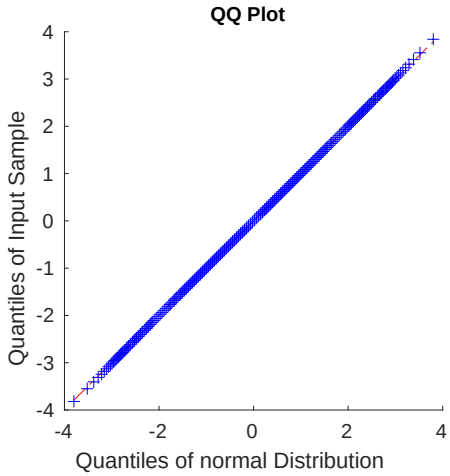

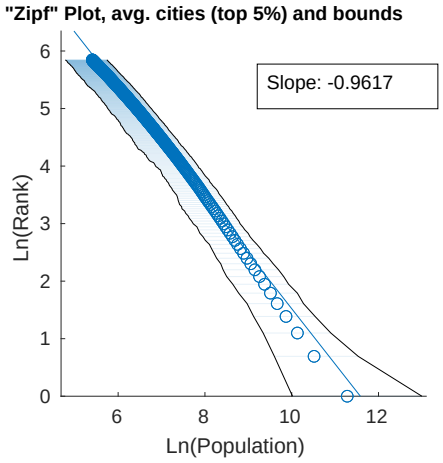

1000-draw MC	Value
Coef. of Avg.	-.962
Avg. over Coefs	-.958
Std. Dev.	(.055)
Min	-1.138
5pct	-1.053
25pct	-.994
50pct	-.957
75pct	-.921
95pct	-.869
Max	-.797

Notes: The population distribution resulting from numerical simulation of model with "effective" distance is in the upper left panel, and the resulting QQ plot is on the upper right. Both show that the equilibrium population distribution appears lognormal. The city size distribution of the Monte Carlo output is in the lower left, and statistics over model simulations the lower right. The slope on the lower left left represents the slope taken over the average of log(pop) at each rank over 1000 simulations, and the bounds contain 95% of the log populations at each rank of the distribution. The table displays statistics over the 1000 estimated power law coefficients from the simulations.

Appendix References

Allen, T. and Arkolakis, C. (2014). Trade and the Topography of the Spatial Economy. *Quarterly Journal of Economics*, 129(3):1085–1140.

Anderson, G., Guionnet, A., and Zeitouni, O. (2010). *An Introduction to Random Matrices*. Cambridge Studies in Advanced Mathematics. Cambridge University Press.

Ben Arous, G. and Guionnet, A. (2010). *Wigner matrices*, pages 433–451. Oxford University Press.

Billingsley, P. (1995). *Probability and Measure*. Wiley Series in Probability and Statistics. Wiley.

Bradley, R. C. (1993). Equivalent mixing conditions for random fields. *The Annals of Probability*, 21(4):1921–1926.

Bradley, R. C. (2005). Basic Properties of Strong Mixing Conditions. A Survey and Some Open Questions. *Probability Surveys*, 2(N.A.).

Dingel, J. I., Miscio, A., and Davis, D. R. (2021). Cities, lights, and skills in developing economies. *Journal of Urban Economics*, 125:103174.

Doukhan, P. (1994). *Mixing: Properties and Examples*. Lecture notes in statistics. 3Island Press.

Eeckhout, J. (2004). Gibrat's Law for (All) Cities. *American Economic Review*, pages 1429–1451.

Gibrat, R. (1931). *Les inégalités économiques*. Paris: Librairie du Recueil Sirey.

Henderson, J. V., Squires, T., Storeygard, A., and Weil, D. (2018). The Global Distribution of Economic Activity: Nature, History, and the Role of Trade. *The Quarterly Journal of Economics*, 133(1):357–406.

Marlow, N. (1967). A Normal Limit Theorem for Power Sums of Independent Random Variables. *Bell System Technical Journal*, 46(9):2081–2089.

Mazmanyan, L., Ohanyan, V., and Treitsch, D. (2008). The Lognormal Central Limit Theorem for Positive Random Variables. *Working Paper*.

Nunn, N. and Puga, D. (2012). Ruggedness: The Blessing of Bad Geography in Africa. *Review of Economics and Statistics*, 94(1):20–36.

O'Rourke, S., Vu, V., and Wang, K. (2016). Eigenvectors of random matrices: A survey. *Journal of Combinatorial Theory, Series A*, 144:361–442.